Inorganic Chemistry

Article

Sila-Substitution of Alkyl Nitrates: Synthesis, Structural Characterization, and Sensitivity Studies of Highly Explosive (Nitratomethyl)-, Bis(nitratomethyl)-, and Tris(nitratomethyl)silanes and Their Corresponding Carbon Analogues

Camilla Evangelisti,[†] Thomas M. Klapötke,*,[†] Burkhard Krumm,[†] Anian Nieder,[†] Raphael J. F. Berger,[‡] Stuart A. Hayes,[‡] Norbert W. Mitzel,*,[‡] Dennis Troegel,[§] and Reinhold Tacke*,[§]

[†]*Department of Chemistry, Ludwig Maximilians University of München, Butenandtstrasse 5−13 (D), D-81377 München, Germany,* [‡]*Faculty of Chemistry, University of Bielefeld, Universitätsstrasse 25, D-33615 Bielefeld, Germany, and* [§]*Institute of Inorganic Chemistry, University of Würzburg, Am Hubland, D-97074 Würzburg, Germany*

A series of analogous nitratomethyl compounds of carbon and silicon of the formula types $Me_3ElCH_2ONO_2$ (**1a/1b**), $Me_2El(CH_2ONO_2)_2$ (**2a/2b**), $MeEl(CH_2ONO_2)_3$ (**3a/3b**), $(CH_2)_4El(CH_2ONO_2)_2$ (**4a/4b**), and $(CH_2)_5El(CH_2ONO_2)_2$ (**5a/5b**) were synthesized [El = C (**a**), Si (**b**); $(CH_2)_4El$ = (sila)cyclopentane-1,1-diyl; $(CH_2)_5El$ = (sila)cyclohexane-1,1-diyl]. All compounds were characterized by using NMR, IR, and Raman spectroscopy and mass spectrometry. In addition, the crystal structures of $Me_2C(CH_2ONO_2)_2$ (**2a**), $(CH_2)_4C(CH_2ONO_2)_2$ (**4a**), $Me_2Si(CH_2ONO_2)_2$ (**2b**), and $(CH_2)_5Si(CH_2ONO_2)_2$ (**5b**) were determined by single-crystal X-ray diffraction. The gas-phase structures of the C/Si analogues **1a** and **1b** were determined by electron diffraction and compared with the results of quantum chemical calculations at different levels of theory. The thermal stabilities of the C/Si pairs **1a/1b**−**5a/5b** were investigated by using DSC. In addition, their friction and impact sensitivities were measured with standard BAM methods. The extreme sensitivities of the silicon compounds **1b**−**5b** compared to those of the corresponding carbon analogues **1a**−**5a** were discussed in terms of the structures of the C/Si analogues and possible geminal Si···O interactions.

Introduction

Alkyl nitrates are well-known compounds, and they are used in many different applications such as drugs, propellants, or explosives.[1,2] Since Alfred Nobel tamed nitroglycerin with kieselguhr, highly sensitive alkyl nitrates have become manageable for industrial, military, and civil purposes.[2] One of the routinely used alkyl nitrates is pentaerythrityl tetranitrate (PETN), $C(CH_2ONO_2)_4$, as a primary explosive. A derivative also bearing a neopentane backbone is 1,1,1-tris-(nitratomethyl)ethane (also known as metriol trinitrate, **3a**; Scheme 1), which is used as an alternative to nitroglycerin in propellant and explosive formulations.[2]

The characteristic of an explosive reaction is a fast propagating decomposition via a shock-wave mechanism. In the case of alkyl nitrate based explosives, the homolytic bond cleavage of the $O−NO_2$ group is mostly the first chemical step of decomposition, followed by ignition, growth of deflagration, and transition from deflagration to detonation. This initial chemical step can be initiated by different external stimuli, like shock, friction, heat, or electrostatic discharge. In some circumstances, the ignition can lead directly to detonation.[2,3]

The first sila-analogues of alkyl nitrates (C/Si exchange) were reported in 1964,[4] along with the syntheses of related compounds of the formula type $R_3ElCHClCH_2ONO_2$ (El = Si, Sn)[4] and organosiloxane-based nitrates obtained from the corresponding silanols of the formula type $(HO)_nSi(CHCl-CH_2ONO_2)_{4−n}$ (n = 2, 3).[5] The first synthesis of a silicon analogue of an alkyl nitrate with a neopentane backbone was described in a patent,[6] where the use of $Me_3SiCH_2ONO_2$ (**1b**, Scheme 1) was claimed as an alternative to nitroglycerin for medical applications, and the explosive behavior of this

---

(1) Boschan, R.; Merrow, R. T.; van Dolah, R. W. *Chem. Rev.* **1955**, *55*, 485–510.
(2) (a) Meyer, R.; Köhler, J.; Homburg, A. *Explosives*, 5th ed.; Wiley-VCH: Weinheim, 2002; pp 216−217. (b) Klapötke, T. M. *Chemie der hochenergetischen Materialien*; de Gruyter: Berlin, 2009; pp 1−6.
(3) (a) Hiskey, M. A.; Brower, K. R.; Oxley, J. C. *J. Phys. Chem.* **1991**, *95*, 3955–3960. (b) Akhavan, J. *The Chemistry of Explosives*; The Royal Society of Chemistry: Cambridge, 1998; pp 63−67. (c) Klapötke, T. M. *Chemie der hochenergetischen Materialien*; de Gruyter: Berlin, 2009; pp 87−88.
(4) Fink, W. U.S. Patent 3,127,431, March 31, **1964**.
(5) Fink, W. U.S. Patent 3,222,319, December 7, **1965**.
(6) Barcza, S. U.S. Patent 3,592,831, July 13, **1971**.

Scheme 1. Carbon/Silicon Analogues **1a/1b−5a/5b** with Various Numbers of Nitratomethyl Groups Bound to the Central Carbon or Silicon Atom

1a: El = C
1b: El = Si

2a: El = C
2b: El = Si

3a: El = C
3b: El = Si

4a: El = C
4b: El = Si

5a: El = C
5b: El = Si
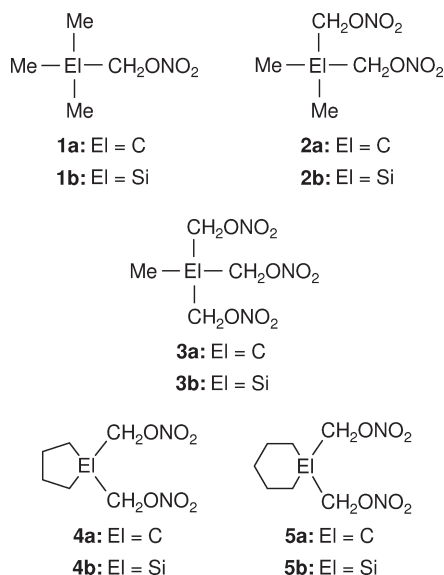
compound was recognized, with possible applications as an energetic material.

Recently, the extremely impact- and friction-sensitive silicon analogue of PETN [C(CH$_2$ONO$_2$)$_4$], sila-PETN (Si(CH$_2$ONO$_2$)$_4$), was synthesized.[7] The first studies of its outstanding sensitivity compared to its carbon analogue PETN were performed and different decomposition pathways of the C/Si analogues C(CH$_2$ONO$_2$)$_4$ and Si-(CH$_2$ONO$_2$)$_4$ were investigated by using quantum chemical methods.[7,8]

To study the characteristics and the reasons for the high instability of (nitratomethyl)silanes, several silicon compounds of this type with various numbers of nitratomethyl groups and their corresponding carbon analogues, the C/Si pairs **1a/1b−5a/5b** (Scheme 1), were synthesized and characterized, including their friction and impact sensitivities. The synthetic access to the precursors of the aforementioned (nitratomethyl)silanes, the corresponding (hydroxymethyl)- and (iodomethyl)silanes, and related compounds with SiCH$_2$X groups (X = Cl, Br, N$_3$, SH) has been discussed extensively.[9−16] The studies on the sila-explosives reported

here represent a logical extension of related investigations dealing with sila-drugs[17] and sila-odorants.[18]

Experimental Section

*Caution! Many alkyl nitrates are sensitive and represent energetic materials; therefore, they must be handled with care! Since sila-analogues of alkyl nitrates are even more sensitive toward shock and friction, they must be manipulated **very** cautiously! During the work with alkyl nitrates, and especially with their sila-analogues, wearing leather jacket, face shield, steel-reinforced Kevlar gloves, ear protection, and electrically grounded shoes is mandatory. Only electrically grounded and metal-free equipment was used during the syntheses.*

Materials. Nitric acid (100%, fuming), Me$_3$SiCH$_2$OH, Me$_3$-SiCH$_2$I, Me$_2$Si(CH$_2$Cl)$_2$, acetonitrile (Aldrich), MeC(CH$_2$OH)$_3$, acetic anhydride (Acros Organics), Me$_3$CCH$_2$OH (Aldrich and Acros Organics), and silver nitrate (VWR) were used as received.

General Remarks. The ^{1}H, ^{13}C{^{1}H}, ^{14}N, and ^{29}Si{^{1}H} NMR spectra were recorded using a Jeol 400 eclipse FT-NMR spectrometer (compounds **1a/b−5a/b**) operating at 400.2 MHz (^{1}H), 100.6 MHz (^{13}C), 28.9 MHz (^{14}N), and 79.5 MHz (^{29}Si) or a Bruker DRX-300 NMR spectrometer (compounds **6−11**) operating at 300.1 MHz (^{1}H), 75.5 MHz (^{13}C), and 59.6 MHz (^{29}Si). Chemical shifts (ppm) are given with respect to TMS (^{1}H, ^{13}C, ^{29}Si; δ 0) and MeNO$_2$ (^{14}N; δ 0) as external standards (compounds **1a/b−5a/b**) or relative to internal [D$_5$]DMSO (^{1}H, δ 2.49; [D$_6$]DMSO), internal [D$_6$]DMSO (^{13}C, δ 39.5; [D$_6$]-DMSO), internal CHCl$_3$ (^{1}H, δ 7.24; CDCl$_3$), internal CDCl$_3$ (^{13}C, δ 77.0; CDCl$_3$), or external TMS (^{29}Si, δ 0; [D$_6$]DMSO, CDCl$_3$) (compounds **6−11**). Analysis and assignment of the ^{1}H NMR data of **6−11** were supported by ^{1}H,^{1}H COSY, ^{13}C,^{1}H HMQC, and ^{13}C,^{1}H HMBC experiments, and assignment of the ^{13}C NMR data was supported by DEPT135, ^{13}C,^{1}H HMQC, and ^{13}C,^{1}H HMBC experiments. Infrared (IR) spectra were recorded on a Perkin-Elmer Spectrum BXII FT-IR instrument equipped with a Diamant-ATR Dura Sampler at 25 °C. Raman spectra were recorded on a Perkin-Elmer Spectrum 2000R NIR FT-Raman instrument equipped with a Nd:YAG laser (1064 nm) with 300 mW at 25 °C, except for compound **3b**; the Raman data of **3b** were collected using a Isa Jobin-Yvon T64000 Raman instrument with CCD detector (EEV CCD115−11) equipped with a Spectra Physics Ar$^+$ laser (514.5 nm) with 30 mW at 25 °C. Melting, boiling, and decomposition points were determined by differential scanning calorimetry (DSC; Perkin-Elmer Pyris 6 DSC, calibrated by standard pure indium and zinc). Measurements were performed at a heating rate of

(7) Klapötke, T. M.; Krumm, B.; Ilg, R.; Troegel, D.; Tacke, R. *J. Am. Chem. Soc.* **2007**, *129*, 6908–6915.

(8) Liu, W.-G.; Zybin, S. V.; Dasgupta, S.; Klapötke, T. M.; Goddard, W. A., III *J. Am. Chem. Soc.* **2009**, *131*, 7490–7491.

(9) Kobayashi, T.; Pannell, K. H. *Organometallics* **1991**, *10*, 1960–1964.

(10) Anderson, W. K.; Kasliwal, R.; Houston, D. M.; Wang, Y.; Narayanan, V. L.; Haugwitz, R. D.; Plowman, J. *J. Med. Chem.* **1995**, *38*, 3789–3797.

(11) Daiss, J. O.; Barth, K. A.; Burschka, C.; Hey, P.; Ilg, R.; Klemm, K.; Richter, I.; Wagner, S. A.; Tacke, R. *Organometallics* **2004**, *23*, 5193–5197.

(12) Ilg, R.; Troegel, D.; Burschka, C.; Tacke, R. *Organometallics* **2006**, *25*, 548–551.

(13) Daiss, J. O.; Burschka, C.; Mills, J. S.; Montana, J. G.; Showell, G. A.; Warneck, J. B. H.; Tacke, R. *Organometallics* **2006**, *25*, 1188–1198.

(14) Shimizu, M.; Iwakubo, M.; Nishihara, Y.; Oda, K.; Hiyama, T. *ARKIVOC* **2007**, 29–48.

(15) Troegel, D.; Möller, F.; Burschka, C.; Tacke, R. *Organometallics* **2009**, *28*, 5765–5770.

(16) Apfel, U.-P.; Troegel, D.; Halpin, Y.; Tschierlei, S.; Uhlemann, U.; Schmitt, M.; Popp, J.; Görls, H.; Dunne, P.; Venkatesan, M.; Coey, M.; Rudolph, M.; Vos, J. G.; Tacke, R.; Weigand, W., manuscript in preparation.

(17) Recent publications dealing with sila-drugs: (a) Büttner, M. W.; Burschka, C.; Daiss, J. O.; Ivanova, D.; Rochel, N.; Kammerer, S.; Peluso-Iltis, C.; Bindler, A.; Gaudon, C.; Germain, P.; Moras, D.; Gronemeyer, H.; Tacke, R. *ChemBioChem* **2007**, *8*, 1688–1699. (b) Tacke, R.; Popp, F.; Müller, B.; Theis, B.; Burschka, C.; Hamacher, A.; Kassack, M. U.; Schepmann, D.; Wünsch, B.; Jurva, U.; Wellner, E. *ChemMedChem* **2008**, *3*, 152–164. (c) Warneck, J. B.; Cheng, F. H. M.; Barnes, M. J.; Mills, J. S.; Montana, J. G.; Naylor, R. J.; Ngan, M.-P.; Wai, M.-K.; Daiss, J. O.; Tacke, R.; Rudd, J. A. *Toxicol. Appl. Pharmacol.* **2008**, *232*, 369–375. (d) Lippert, W. P.; Burschka, C.; Götz, K.; Kaupp, M.; Ivanova, D.; Gaudon, C.; Sato, Y.; Antony, P.; Rochel, N.; Moras, D.; Gronemeyer, H.; Tacke, R. *ChemMedChem* **2009**, *4*, 1143–1152. (e) Tacke, R.; Müller, V.; Büttner, M. W.; Lippert, W. P.; Bertermann, R.; Daiss, J. O.; Khanwalkar, H.; Furst, A.; Gaudon, C.; Gronemeyer, H. *ChemMedChem* **2009**, *4*, 1797–1802. (f) Johansson, T.; Weidolf, L.; Popp, F.; Tacke, R.; Jurva, U. *Drug Metab. Dispos.* **2010**, *38*, 73–83. (g) Tacke, R.; Nguyen, B.; Burschka, C.; Lippert, W. P.; Hamacher, A.; Urban, C.; Kassack, M. U. *Organometallics* **2010**, *29*, 1652−1660.

(18) Recent publications dealing with sila-odorants: (a) Büttner, M. W.; Burschka, C.; Junold, K.; Kraft, P.; Tacke, R. *ChemBioChem* **2007**, *8*, 1447–1454. (b) Büttner, M. W.; Nätscher, J. B.; Burschka, C.; Tacke, R. *Organometallics* **2007**, *26*, 4835–4838. (c) Tacke, R.; Metz, S. *Chem. Biodiversity* **2008**, *5*, 920–941. (d) Metz, S.; Nätscher, J. B.; Burschka, C.; Götz, K.; Kaupp, M.; Kraft, P.; Tacke, R. *Organometallics* **2009**, *28*, 4700–4712. (e) Nätscher, J. B.; Laskowski, N.; Kraft, P.; Tacke, R. *ChemBioChem* **2010**, *11*, 315–319.

β = 5 °C in closed aluminum containers with a hole (1 μm) on the top for gas release with a nitrogen flow of 5 mL/min. The reference sample was an closed aluminum container with air. Friction and impact sensitivities were determined by standard BAM methods.[19] A Büchi GKR-51 apparatus was used for the bulb-to-bulb distillations of **9−11**. The melting points of **7** and **8** were determined with a Büchi Melting Point B-540 apparatus using samples in sealed glass capillaries. The crystal structures were determined by using an Oxford Xcalibur CCD diffractometer (compounds **2a**, **2b**, **4a**, and **5b**) or a Stoe IPDS diffractometer (compounds **7** and **8**) and graphite-monochromated Mo−K$_\alpha$ radiation (λ = 0.71073 Å). The structures were solved with SHELXS-97 and were refined with SHELXL-97,[21] implemented in the program package WinGX[22] and finally checked using Platon.[23] Elemental analyses of the nitratomethyl compounds were not performed because of their highly sensitive and explosive properties. Mass spectrometric data were obtained from a Jeol Mstation JMS 700 spectrometer, except for **2b** and **3b**, which were too hazardous.

Gas Electron Diffraction (GED). Electron scattering intensities were recorded at room temperature on a combination of reusable Fuji and Kodak imaging plates using a Balzers KD-G2 Gas-Eldigraph[24] (formerly operated in Tübingen by H. Oberhammer[25]). This has been equipped with an electron source built by STAIB Instruments, which was operated at 60 kV (**1a**) or 70 kV (**1b**). The accelerating voltage was monitored using a 0 to 10 V signal generated by the high-voltage supply, proportional to the variable 0 to 100 kV output, which was stable to within 0.1 to 0.2 mV during the course of the experiment. The image plates were scanned using a Fuji BAS 1800 scanner, yielding digital 16-bit gray scale image data. Further details about the Bielefeld GED apparatus and the experimental method are published elsewhere.[26]

In preparation for data reduction, the long and short nozzle-to-plate distances were remeasured after recording the short-distance data and before recording the long-distance data for **1a**. The relative scaling of the two scanning directions was also recalibrated by using an exposed image plate with two pairs of pin holes, which was scanned in two orientations, approximately perpendicular to one another. The data were reduced to total intensities using Strand et al.'s program PIMAG[27] (version 040827) in connection with a sector curve, which was based on experimental xenon scattering data and tabulated scattering factors of xenon. Further data reduction yielding molecular-intensity curves was performed by using version 2.4 of the ed@ed program,[28] using the scattering factors of Ross et al.[29] For both compounds the ratio of the electron wavelength to the nozzle-to-plate distances was checked using benzene data and the widely accepted r_a value of 1.397 Å for the C−C distance in benzene. In the determination of **1a**, the calculated electron wavelength was assumed to be correct, and the nozzle-to-plate distances were checked for consistency with the measured values leading to a small scaling being applied to the long distance. For **1b**, the data reduction was performed using the previously measured nozzle-to-plate distances, and a small scaling was applied to the electron wavelength for the data set recorded at the short distance. The electron wavelengths and nozzle-to-plate distances are provided as Supporting Information, along with other data analysis parameters including the s-limits, weighting points, R factors (R_D and R_G), scale factors, data correlation values, and the correlation matrix.

The amplitudes of vibration, u, used in the r_g and r_{h1} refinements, and the distance corrections for curvilinear perpendicular motion, k_{h1}, were calculated by using the program SHRINK.[30,31] This made use of frequency calculations for **1a** and **1b**, respectively, at the RI-MP2/TZVPP and HF/6-31G* level of theory (for details of calculations, see below). The SHRINK input file for **1b** was generated using EasyInp written by K. B. Borisenko, while that for **1a** was generated using a combination of EasyInp and Q2SHRINK,[32] written by A. Zakharov.

Theoretical Calculations. All Hartree−Fock (HF) calculations were of the restricted type, and the second-order Møller−Plesset (MP2) calculations made use of the resolution-of-the-identity (RI) method and the default frozen-core partitioning as implemented in Turbomole.[33] The HF calculations using the Pople-style 6-31G* basis sets were performed by using the default criteria in Gaussian 03,[34a] while those using the def2-TZVPP (herein shortened to TZVPP) basis set were performed by using Turbomole.

The theoretical calculations for structure optimization of **2a** and **2b** were performed at the B3LYP level of theory (cc-pVDZ basis sets) using Gaussian 03,[34b] and the NBO analyses were performed using the Gaussian 03 nbo5-tool. Instead, the calculations of the enthalpies of formation were performed at the CBS-4 M level of theory.

General Procedure for the Nitration of the (Hydroxymethyl)-alkanes and (Hydroxymethyl)cycloalkanes. For the synthesis of **1a**, **2a**, **4a**, and **5a**, the respective hydroxymethyl or bis(hydroxymethyl) compound [Me$_3$CCH$_2$OH, Me$_2$C(CH$_2$OH)$_2$, (CH$_2$)$_4$-C(CH$_2$OH)$_2$, (CH$_2$)$_5$C(CH$_2$OH)$_2$; 1.0 mmol (1.0 mol equiv)] was added in small portions at 20 °C to a stirred mixture of nitric acid (100%; 2.1 and 4.2 mol equiv, respectively) and acetic anhydride (6.0 mol equiv). [For the synthesis of **3a**, the tris-(hydroxymethyl) compound MeC(CH$_2$OH)$_3$ was added in small portions at 0 °C to a stirred mixture of nitric acid (100%; 3.3 mol equiv) and dichloromethane (5 mL).] The reaction mixture was then stirred at ambient temperature for 1.5 (**1a**, **2a**, **4a**, **5a**) or 2 h (**3a**), followed by the addition of ice−water (5 mL) and pentane (15 mL). The aqueous phase was separated and extracted with pentane (2 × 20 mL), and the combined organic extracts were washed with water (2 × 20 mL), neutralized by washing with a concentrated aqueous solution of sodium hydrogen carbonate, and then dried over anhydrous sodium sulfate. The solvent was removed under reduced pressure, and the residue was purified by distillation (**1a**) or by removal of the remaining solvent traces in vacuo (0.01 mbar, 20 °C, 3−6 h) (**2a**−**5a**). For further details of the syntheses, see Table 1.

2,2-Dimethyl-1-nitratopropane, Me$_3$CCH$_2$ONO$_2$ (1a). The crude product was distilled in vacuo (60 °C/50 mbar) to give

(19) (a) http://www.bam.de/index_en.html. (b) *Official Journal of the European Union,* Council Regulation (EC) No. 440/2008, 30th of March **2008**.

(20) Hylands, K. A.; Moodie, R. B. *J. Chem. Soc., Perkin Trans. 2* **1997**, 709−714.

(21) Sheldrick, G. M. *SHELXL-97, A program for the refinement of crystal structures*; University of Göttingen: Göttingen, Germany, 1994.

(22) Farrugia, L. J. *WinGX, J. Appl. Crystallogr.* **1999**, *32*, 837−838.

(23) Spek, A. L. *Platon*; Utrecht University: Utrecht, The Netherlands, 1999.

(24) Zeil, W.; Haase, J.; Wegmann, L. *Z. Instrum.* **1966**, *74*, 84−88.

(25) Oberhammer, H. In *Molecular Structure by Diffraction Methods*; Sim, G. A, Sutton, L. E., Eds.; The Chemical Society: London, 1976; Vol. *4*, pp 24−44.

(26) Berger, R. J. F.; Mitzel, N. W. *Z. Naturforsch.* **2009**, *64b*, 1259−1268.

(27) Gundersen, S.; Samdal, S.; Strand, T. G.; Volden, H. V. *J. Mol. Struct.* **2007**, *832*, 164−171.

(28) Hinchley, S. L.; Robertson, H. E.; Borisenko, K. B.; Turner, A. R.; Johnston, B. F.; Rankin, D. W. H.; Ahmadian, M.; Jones, J. N.; Cowley, A. H. *Dalton Trans.* **2004**, 2469−2476.

(29) Ross, A. W.; Fink, M.; Hilderbrandt, R. In *International Tables for Crystallography*; Wilson, A. C. J., Ed.; Kluwer Academic Publishers: Dordrecht, The Netherlands, 1992; Vol. *C*, pp 245−338.

(30) Sipachev, V. A. *J. Mol. Struct., THEOCHEM* **1985**, *121*, 143−151.

(31) Novikov, V. P.; Sipachev, V. A.; Kulikova, E. I.; Vilkov, L. V. *J. Mol. Struct.* **1993**, *301*, 29−36.

(32) Zakharov, A. V. *Q2SHRINK*, version 1.3; http://edsoftware.sourceforge.net.

(33) *Turbomole*, version 5.7; Ahlrichs, R.; Bär, M.; Häser, M.; Horn, H.; Kölmel, C. *Chem. Phys. Lett.* **1989**, *162*, 165−169.

(34) (a) Frisch, M. J. et al. *Gaussian 03*, revision C.02; Gaussian, Inc.: Wallingford, CT, 2004. (b) Frisch, M. J. et al. *Gaussian 03*, revision D.01; Gaussian, Inc.: Wallingford, CT, 2004.

Table 1. Nitration Procedures, Molar Equivalents of the Nitration Agent HNO_3, and Reaction Times for the Syntheses of the Carbon-Based Nitratomethyl Compounds **1a−5a** as well as Yields and Melting, Boiling, and Decomposition Points of **1a−5a**

compound	1a	2a	3a	4a	5a
nitration agents	HNO_3/Ac_2O	HNO_3/Ac_2O	$HNO_3 (CH_2Cl_2)$	HNO_3/Ac_2O	HNO_3/Ac_2O
molar equivalents of nitric acid [a]	2.1	4.2	6.3	4.2	4.2
reaction time [h]	1.5	1.5	2.0	1.5	1.5
% yield	88	82	86	83	86
mp./bp. [°C] [b]	-/174	18−23/178 [b]	−15/182 [b]	23−25/190 [b]	-/190 [b]

[a] Calculated for 1.0 mol equiv of the starting material. [b] Decomposition.

Table 2. Nitration Procedures (Methods A and B), Molar Equivalents of the Nitration Agent, and Reaction Times for the Syntheses of the Silicon-Based Nitratomethyl Compounds **1b−5b** as well as Yields and Melting, Boiling, and Decomposition Points of **1b−5b**

compound	1b	2b	3b	4b	5b
nitration procedure	B	A	A	A	A
molar equivalents of nitration agent[a]	2.0	4.2	6.3	4.2	4.2
reaction time [h]	1.5	1.0	1.5	1.5	1.5
% yield	86	87	80	94	96
mp./bp. [°C][b]	-/85[b]	−10/107[b]	∼ −18/107[b]	∼ −18/97[b]	∼ 4/96[b]

[a] Calculated for 1.0 mol equiv of the starting material. [b] Decomposition.

1a 88% yield as a colorless liquid. NMR (CDCl$_3$): ^{1}H, δ 0.97 (s, 9 H, CCH_3), 4.12 (s, 2 H, CCH_2O); ^{13}C, δ 26.4 (CCH_3), 31.4 (C_q), 82.1 (CCH_2O); ^{14}N, δ −41.2. Raman (300 mW): 2968 (vs), 2910 (vs), 2796 (w), 1629 (w), 1460 (m), 1365 (w), 1280 (s), 1261 (m), 1261 (w), 1045 (vw), 975 (vw), 921 (m), 868 (m), 769 (s), 696 (w), 611 (m), 478 (m), 405 (vw) cm^{-1}. IR: 2963 (w), 2875 (vw), 1621 (vs), 1479 (vw), 1467 (w), 1279 (vs), 1219 (vw), 1043 (vw), 976 (w), 943 (vw), 924 (vw), 865 (m), 847 (m), 759 (vw), 694 (vw), 638 (vw) cm^{-1}. MS (DEI+) [m/e]: 133.1 [M$^+$]. Bp.: 174 °C. Sensitivities: impact, > 100 J; friction, > 360 N.

2,2-Dimethyl-1,3-dinitratopropane, Me$_2$C(CH$_2$ONO$_2$)$_2$ (2a). The crude product was dried in vacuo (0.01 mbar, 25 °C, 3 h) to give **2a** in 82% yield as a colorless liquid. NMR (CDCl$_3$): ^{1}H, δ 1.08 (s, 6 H, CCH_3), 4.26 (s, 4 H, CCH_2O); ^{13}C, δ 22.1 (CCH_3), 34.7 (C_q), 76.5 (CCH_2O); ^{14}N, δ −44.5. Raman (300 mW): 2969 (vs), 2910 (s), 2808 (vw), 2732 (vw), 1635 (w), 1467 (m), 1403 (vw), 1372 (w), 1285 (s), 1032 (w), 982 (vw), 921 (w), 870 (s), 795 (w), 693 (w), 608 (m), 475 (m), 408 (vw) cm^{-1}. IR: 2977 (w), 2900 (vw), 1826 (w), 1755 (vw), 1623 (vs), 1477 (w), 1369 (m), 1268 (vs), 1230 (w), 1122 (m), 1032 (w), 977 (s), 943 (w), 923 (w), 843 (vs), 756 (s), 718 (w), 703 (w), 637 (w) cm^{-1}. MS (DEI-) [m/e]: 193.1 [M − H]$^-$. Mp.: 18−23 °C. Bp.: 178 °C (dec.). Sensitivities: impact > 100 J; friction > 96 N.

2-Methyl-2-nitratomethyl-1,3-dinitratopropane, MeC(CH$_2$ONO$_2$)$_3$ (3a). The crude product was dried in vacuo (0.01 mbar, 25 °C, 6 h) to give **3a** in 86% yield as a colorless viscous liquid. NMR (CDCl$_3$): ^{1}H, δ 1.08 (s, 3 H, CCH_3), 4.26 (s, 6 H, CCH_2O); ^{13}C, δ 22.1 (CCH_3), 34.7 (C_q), 76.5 (CCH_2O); ^{14}N, δ −44.5. Raman (300 mW): 2972 (vs), 2910 (m), 2802 (vw), 2738 (vw), 1641 (m), 1467 (m), 1407 (vw), 1374 (w), 1286 (vs), 1036 (w), 994 (vw), 918 (vw), 869 (s), 639 (m), 601 (m), 465 (w), 414 (w) cm^{-1}. IR: 2962 (vw), 2907 (vw), 1825 (vw), 1753 (vw), 1626 (vs), 1473 (w), 1374 (w), 1271 (vs), 1124 (m), 1031 (w), 990 (s), 923 (w), 835 (vs), 752 (s), 724 (m), 704 (m) cm^{-1}. MS (DCI+) [m/e]: 256.1 [M + H]$^+$. Mp.: −15 °C (ref 2: −15 °C). Bp.: 182 °C (dec.) (ref 2: 182 °C). Sensitivities: impact > 15 J; friction > 108 N.

1,1-Bis(nitratomethyl)cyclopentane, (CH$_2$)$_4$C(CH$_2$ONO$_2$)$_2$ (4a). The crude product was dried in vacuo (0.01 mbar, 25 °C, 3 h) to give **4a** in 83% yield as a colorless liquid. NMR (CDCl$_3$): ^{1}H, δ 1.57−1.62 (m, 4 H, β-CH_2), 1.67−1.72 (m, 4 H, γ-CH_2), 4.33 (s, 4 H, CCH_2O); ^{13}C, δ 24.9 (γ-CH_2), 32.8 (β-CH_2), 44.8 (C_q), 75.0 (CCH_2O); ^{14}N, δ −43.9. Raman (300 mW): 2967 (vs), 2877 (s), 1635 (w), 1454 (m), 1384 (vw), 1284 (s), 1239 (w), 1029 (w), 991 (vw), 906 (m), 869 (s), 703 (w), 607 (m), 471 (w) cm^{-1}. IR: 2958 (w), 2874 (vw), 1728 (m), 1622 (vs), 1453 (w), 1370 (vw), 1338 (vw), 1272 (vs), 1166 (w), 1130 (vw), 1024 (vw), 990 (m), 956 (w), 851 (vs), 755 (s), 700 (w), 668 (vw), 637 (vw) cm^{-1}. MS (DEI+) [m/e]:

222.3 [M + 2H]$^+$. Mp.: 23−25 °C. Bp.: 190 °C (dec.). Sensitivities: impact > 100 J; friction > 108 N.

1,1-Bis(nitratomethyl)cyclohexane, (CH$_2$)$_5$C(CH$_2$ONO$_2$)$_2$ (5a). The crude product was dried in vacuo (0.01 mbar, 25 °C, 3 h) to give **5a** in 86% yield as a colorless liquid. NMR (CDCl$_3$): ^{1}H, δ 1.45−1.55 (m, 10 H, CCH_2C), 4.37 (s, 4 H, CCH_2O); ^{13}C, δ 20.9 (γ-CH_2), 25.5 (δ-CH_2), 29.9 (β-CH_2), 37.2 (C_q), 74.5 (CCH_2O); ^{14}N, δ −43.5. Raman (300 mW): 2946 (vs), 2864 (s), 1635 (w), 1473 (w), 1447 (m), 1388 (vw), 1365 (w), 1283 (s), 1251 (w), 1030 (w), 988 (w), 867 (s), 852 (s), 833 (m), 684 (vw), 606 (m), 475 (m) cm^{-1}. IR: 2936 (w), 2862 (vw), 1622 (vs), 1455 (w), 1371 (vw), 1316 (vw), 1280 (vs), 1267 (vs), 1078 (vw), 1018 (vw), 988 (m), 930 (m), 930 (w), 843 (vs), 755 (s), 702 (m), 684 (vw), 636 (w) cm^{-1}. MS (DEI+) [m/e]: 235.2 [M + H]$^+$. Bp.: 190 °C (dec.). Sensitivities: impact > 100 J; friction, > 120 N.

General Procedure of the Nitration of the (Hydroxymethyl)-silanes and (Hydroxymethyl)silacyloalkanes. Method A. For the synthesis of **2b−5b**, the respective bis(hydroxymethyl) or tris(hydroxymethyl) compound [Me$_2$Si(CH$_2$OH)$_2$, MeSi-(CH$_2$OH)$_3$, (CH$_2$)$_4$Si(CH$_2$OH)$_2$, (CH$_2$)$_5$Si(CH$_2$OH)$_2$; 1.0 mmol (1.0 mol equiv)] was added in small portions to a stirred mixture of nitric acid (100%; 4.2 and 6.3 mol equiv, respectively) and acetic anhydride (6.0 mol equiv). The reaction mixture was stirred at ambient temperature for 1 h (**2b**) or 1.5 h (**3b−5b**), followed by the addition of ice−water (5 mL) and pentane (15 mL). The aqueous phase was separated and extracted with pentane (2 × 20 mL), and the combined organic extracts were washed with water (2 × 20 mL), neutralized by washing with a concentrated aqueous solution of sodium hydrogen carbonate, and then dried over anhydrous sodium sulfate. The solvent was removed under reduced pressure, and the residue was purified by removal of the remaining solvent traces in vacuo (0.01 mbar, 25 °C, 2 h). For further details of the syntheses, see Table 2.

Method B. For the synthesis of **1b**, the respective iodomethyl compound Me$_3$SiCH$_2$I [1.0 mmol (1.0 mol equiv)] was added at 0 °C to a stirred solution of silver nitrate (2.0 mol equiv) in acetonitrile (3 mL). The reaction mixture was then stirred at ambient temperature for 1.5 h under exclusion of light, followed by the addition of pentane (10 mL) under vigorous stirring. The pentane phase was separated, and the extraction procedure with pentane was repeated twice. The pentane extracts were combined, and the solvent was removed by microdistillation (40 °C, 200 mbar). For further details of the synthesis, see Table 2.

Trimethyl(nitratomethyl)silane, Me$_3$SiCH$_2$ONO$_2$ (1b). Compound **1b** was synthesized according to Method B and was isolated in 86% yield as a colorless liquid. NMR (CDCl$_3$): ^{1}H, δ 0.10 (s, 9 H, ^2J(^{1}H,^{29}Si) = 3.4 Hz, SiCH_3), 4.04 (s, 2 H,

$^2J(^1H,^{29}Si)$ = 2.2 Hz, SiCH_2O); ^{13}C, δ −2.8 ($^1J(^{13}C,^{29}Si)$ = 26.5 Hz, SiCH_3), 66.8 ($^1J(^{13}C,^{29}Si)$ = 24.2 Hz, SiCH_2O); ^{14}N, δ −34.3; ^{29}Si, δ 0.1. Raman (300 mW): 2961 (m), 2904 (vs), 1635 (w), 1413 (w), 1305 (m), 1248 (vw), 1213 (vw), 874 (w), 826 (m), 725 (vw), 706 (w), 649 (m), 608 (m), 554 (m) cm^{-1}. IR: 2961 (vw), 1630 (vs), 1436 (vw), 1302 (vs), 1252 (s), 1213 (vw), 977 (vw), 822 (vs), 774 (s), 754 (s), 706 (m) cm^{-1}. MS (DCI+) [m/e]: 149.2 [M$^+$]. Decomp. point: 85 °C. Sensitivities: impact > 1 J; friction > 64 N.

Dimethylbis(nitratomethyl)silane, Me$_2$Si(CH$_2$ONO$_2$)$_2$ (2b). Compound **2b** was synthesized according to Method A and was isolated in 87% yield as a colorless oil. NMR (CDCl$_3$): ^{1}H, δ 0.29 (s, 6 H, $^2J(^1H,^{29}Si)$ = 3.5 Hz, SiCH_3), 4.18 (s, 4 H, $^2J(^1H,^{29}Si)$ = 2.3 Hz, SiCH_2O); ^{13}C, δ −6.0 ($^1J(^{13}C,^{29}Si)$ = 27.7 Hz, SiCH_3), 63.6 ($^1J(^{13}C,^{29}Si)$ = 26.5 Hz, SiCH_2O); ^{14}N, δ −37.6; ^{29}Si, δ −1.2. Raman (300 mW): 2971 (m), 2910 (vs), 2853 (w), 1638 (vw), 1435 (vw), 1305 (m), 1254 (vw), 1213 (vw), 979 (vw), 833 (m), 731 (vw), 671 (m), 646 (vw), 614 (vw), 551 (m) cm^{-1}. IR: 2961 (vw), 2919 (vw), 1724 (vw), 1625 (vs), 1437 (vw), 1405 (vw), 1297 (vs), 1250 (s), 1212 (w), 1163 (vw), 1072 (w), 980 (w), 817 (vs), 752 (m), 670 (m), 641 (m) cm^{-1}. Mp.: −10 °C. Decomp. point: 107 °C. Sensitivities: impact < 0.5 J; friction < 5 N.

Methyltris(nitratomethyl)silane, MeSi(CH$_2$ONO$_2$)$_3$ (3b). Compound **3b** was synthesized according to Method A and was isolated in 80% yield as a colorless oil. NMR (CDCl$_3$): ^{1}H, δ 0.45 (s, 3 H, $^2J(^1H,^{29}Si)$ = 3.6 Hz, SiCH_3), 4.32 (s, 6 H, $^2J(^1H,^{29}Si)$ = 2.3 Hz, SiCH_2O); ^{13}C, δ −8.7 ($^1J(^{13}C,^{29}Si)$ = 28.8 Hz, SiCH_3), 60.7 ($^1J(^{13}C,^{29}Si)$ = 28.1 Hz, SiCH_2O); ^{14}N, δ −40.3; ^{29}Si, δ −5.4. Raman (30 mW): 2972 (s), 2921 (vs), 1639 (w), 1434 (w), 1306 (vs), 1257 (w), 1213 (vw), 989 (w), 839 (vs), 744 (w), 670 (w), 647 (w), 619 (w), 528 (m) cm^{-1}. IR: 2926 (vw),1628 (vs), 1433 (w), 1404 (vw), 1298 (vs), 1253 (s), 1214 (m), 1098 (w), 986 (m), 811 (vs), 746 (s) cm^{-1}. Mp.: ∼ −18 °C. Decomp. point: 107 °C. Sensitivities: impact < 0.5 J; friction < 5 N.

1,1-Bis(nitratomethyl)-1-silacyclopentane, (CH$_2$)$_4$Si(CH$_2$ONO$_2$)$_2$ (4b). Compound **4b** was synthesized according to Method A and was isolated in 94% yield as a colorless oil. NMR (CDCl$_3$): ^{1}H, δ 0.80−0.86 (m, 4 H, β-CH_2), 1.63−1.69 (m, 4 H, γ-CH_2), 4.28 (s, 4 H, $^2J(^1H,^{29}Si)$ = 2.2 Hz, SiCH_2O); ^{13}C, δ 8.2 ($^1J(^{13}C,^{29}Si)$ = 27.3 Hz, β-CH_2), 26.8 (γ-CH_2), 62.4 ($^1J(^{13}C,^{29}Si)$ = 25.8 Hz, SiCH_2O); ^{14}N, δ −37.8; ^{29}Si, δ 13.7. Raman (300 mW): 2942 (vs), 2923 (vs), 2861 (m), 1638 (vw), 1453 (w), 1435 (w), 1407 (w), 1303 (m), 1251 (w), 1210 (vw), 1194 (vw), 1153 (vw), 1080 (vw), 1017 (vw), 979 (vw), 944 (vw), 848 (vs), 705 (w), 655 (w), 611 (vw), 554 (m), 420 (vw) cm^{-1}. IR: 2935 (w), 2863 (vw), 1625 (vs), 1452 (vw), 1431 (vw), 1403 (vw), 1297 (vs), 1250 (s), 1212 (w), 1152 (vw), 1077 (m), 1031 (w), 1018 (w), 977 (w), 814 (vs), 744 (m), 674 (m), 639 (s) cm^{-1}. MS (FAB+) [m/e]: 235.1 [M − H]$^+$. Mp.: ∼ −18 °C. Decomp. point: 97 °C. Sensitivities: impact < 0.5 J; friction < 5 N.

1,1-Bis(nitratomethyl)-1-silacyclohexane, (CH$_2$)$_5$Si(CH$_2$ONO$_2$)$_2$ (5b). Compound **5b** was synthesized according to Method A and was isolated in 96% yield as a colorless oil. NMR (CDCl$_3$): ^{1}H, δ 0.82−0.88 (m, 4 H, β-CH_2), 1.40−1.48 (m, 2 H, δ-CH_2), 1.67−1.77 (m, 4 H, γ-CH_2), 4.24 (s, 4 H, $^2J(^1H,^{29}Si)$ = 2.2 Hz, SiCH_2O); ^{13}C, δ 8.0 ($^1J(^{13}C,^{29}Si)$ = 26.8 Hz, β-CH_2), 23.8 (δ-CH_2), 29.0 (γ-CH_2), 62.2 ($^1J(^{13}C,^{29}Si)$ = 25.9 Hz, SiCH_2O); ^{14}N, δ −37.2; ^{29}Si, δ −6.5. Raman (300 mW): 2923 (vs), 2858 (s), 1641 (vw), 1450 (w), 1403 (vw), 1304 (m), 1213 (vw), 1105 (vw), 1077 (vw), 1008 (vw), 982 (vw), 909 (vw), 838 (m), 796 (w), 666 (m), 608 (vw), 553 (m) cm^{-1}. IR: 2925 (w), 2853 (w), 1718 (vw), 1628 (vs), 1460 (vw), 1447 (vw), 1434 (vw), 1403 (vw), 1297 (vs), 1251 (m), 1210 (vw), 1181 (w), 1101 (vw), 1075 (vw), 993 (w), 977 (w), 910 (m), 832 (s), 801 (s), 752 (s), 641 (s) cm^{-1}. MS (FAB+) [m/e]: 249.2 [M − H]$^+$. Mp.: ∼ 4 °C. Decomp. point: 96 °C. Sensitivities: impact < 0.5 J; friction > 36 N.

General Procedure for the Synthesis of the Bis(hydroxymethyl)silanes 6−8. Catalytic amounts of acetyl chloride were added dropwise at ambient temperature within 1 min to a stirred solution of the respective bis(acetoxymethyl)silane (compounds

9−11) in methanol, and the resulting mixture was heated under reflux for 20 h. The solvent was removed under reduced pressure, and the residue was purified as described in the respective protocols given below.

Bis(hydroxymethyl)dimethylsilane, Me$_2$Si(CH$_2$OH)$_2$ (6). This compound was synthesized from **9** (9.15 g, 44.8 mmol), methanol (400 mL), and acetyl chloride (563 mg, 7.17 mmol). The crude product was purified by fractional distillation using a Vigreux column to give **6** in 73% yield as a colorless liquid (3.96 g, 32.9 mmol). Bp.: 65−66 °C/0.2 mbar. NMR ([D$_6$]DMSO): ^{1}H, δ −0.03 (s, 6 H, SiCH_3), 3.17 (d, $^3J(^1H,^1H)$ = 4.3 Hz, 4 H, SiCH_2O), 3.91 (t, $^3J(^1H,^1H)$ = 4.3 Hz, 2 H, OH); ^{13}C, δ −6.2 (SiCH_3), 51.4 (SiCH_2O); ^{29}Si, δ −2.7. Anal. Calcd for C$_4$H$_{12}$O$_2$Si: C, 39.96; H, 10.06. Found: C, 39.9; H, 9.9.

1,1-Bis(hydroxymethyl)-1-silacyclopentane, (CH$_2$)$_4$Si(CH$_2$OH)$_2$ (7). This compound was synthesized from **10** (3.15 g, 13.7 mmol), methanol (150 mL), and acetyl chloride (142 mg, 1.81 mmol). The crude product was purified by bulb-to-bulb distillation (85 °C/0.03 mbar), and the resulting colorless liquid was crystallized from acetonitrile (4 mL; slow cooling to −20 °C and crystallization over a period of 24 h). The product was isolated by removal of the mother liquor via a syringe and then dried in vacuo (0.2 mbar, 20 °C, 2 h) to give **7** in 60% yield as a colorless crystalline solid (1.20 g, 8.24 mmol). Mp.: 37−38 °C. NMR ([D$_6$]DMSO): ^{1}H, δ 0.53−0.59 (m, 4 H, β-CH_2), 1.49−1.54 (m, 4 H, γ-CH_2), 3.27 (d, $^3J(^1H,^1H)$ = 4.4 Hz, 4 H, SiCH_2O), 3.99 (t, $^3J(^1H,^1H)$ = 4.4 Hz, 2 H, OH); ^{13}C, δ 7.6 (β-CH_2), 26.8 (γ-CH_2), 49.9 (SiCH_2O); ^{29}Si, 14.2. Anal. Calcd for C$_6$H$_{14}$O$_2$Si: C, 49.27; H, 9.65. Found: C, 49.3; H, 9.6.

1,1-Bis(hydroxymethyl)-1-silacyclohexane, (CH$_2$)$_5$Si(CH$_2$OH)$_2$ (8). This compound was synthesized from **11** (6.04 g, 24.7 mmol), methanol (370 mL), and acetyl chloride (558 mg, 7.11 mmol). The crude product was crystallized from acetonitrile (15 mL; slow cooling to −20 °C and crystallization over a period of 24 h). The product was isolated by removal of the mother liquor via a syringe and then dried in vacuo (0.1 mbar, 20 °C, 3 h) to give **8** in 70% yield as a colorless crystalline solid (2.76 g, 17.2 mmol). Mp.: 39−40 °C. NMR ([D$_6$]DMSO): ^{1}H, δ 0.60−0.64 (m, 4 H, β-CH_2), 1.30−1.38 (m, 2 H, δ-CH_2), 1.58−1.67 (m, 4 H, γ-CH_2), 3.25 (d, $^3J(^1H,^1H)$ = 4.4 Hz, 4 H, SiCH_2O), 3.99 (t, $^3J(^1H,^1H)$ = 4.4 Hz, 2 H, OH); ^{13}C, δ 7.9 (β-CH_2), 24.1 (δ-CH_2), 29.5 (γ-CH_2), 49.6 (SiCH_2O); ^{29}Si, −7.7. Anal. Calcd for C$_7$H$_{16}$O$_2$Si: C, 52.45; H, 10.06. Found: C, 52.1; H, 9.8.

General Procedure for the Synthesis of the Bis(acetoxymethyl)silanes 9−11. The respective bis(chloromethyl)silane[16] was added in a single portion at ambient temperature to a stirred suspension of sodium acetate (3 mol equiv) in N,N-dimethylformamide, and the resulting mixture was then stirred under reflux for 18 h. The solvent was removed by distillation (45 °C/10 mbar), diethyl ether (200 mL) and water (200 mL) were added to the residue, the organic layer was separated, and the aqueous phase was extracted with diethyl ether (2 × 200 mL) and then discarded. The combined organic extracts were dried over anhydrous sodium sulfate, the solvent was removed under reduced pressure, and the residue was purified by bulb-to-bulb distillation.

Bis(acetoxymethyl)dimethylsilane, Me$_2$Si(CH$_2$OAc)$_2$ (9). This compound was synthesized from bis(chloromethyl)dimethylsilane[16] (9.00 g, 57.3 mmol), sodium acetate (14.1 g, 172 mmol), and N,N-dimethylformamide (95 mL) to give **9** in 79% yield as a yellowish liquid (9.29 g, 45.5 mmol). Bp.: 55 °C/0.2 mbar. NMR (CDCl$_3$): ^{1}H, δ 0.09 (s, 6 H, SiCH_3), 1.99 (s, 6 H, C(O)CH_3), 3.78 (s, 4 H, SiCH_2O); ^{13}C, δ −6.1 (SiCH_3), 20.6 (C(O)CH_3), 55.3 (SiCH_2O), 171.6 (C(O)CH_3); ^{29}Si, −7.7. Anal. Calcd for C$_8$H$_{16}$O$_4$Si: C, 47.03; H, 7.89. Found: C, 46.8; H, 7.9.

1,1-Bis(acetoxymethyl)-1-silacyclopentane, (CH$_2$)$_4$Si(CH$_2$OAc)$_2$ (10). This compound was synthesized from 1,1-bis(chloromethyl)-1-silacyclopentane[16] (9.13 g, 49.8 mmol), sodium acetate (12.5 g, 152 mmol), and N,N-dimethylformamide (80 mL) to give **10** in

76% yield as a yellowish liquid (8.77 g, 38.1 mmol). Bp.: 85 °C/0.4 mbar. NMR (CDCl$_3$): ^{1}H, δ 0.59−0.64 (m, 4 H, β-CH_2), 1.51−1.56 (m, 4 H, γ-CH_2), 1.98 (s, 6 H, C(O)CH_3), 3.85 (s, 4 H, SiCH_2O); ^{13}C, δ 8.9 (β-CH_2), 20.5 (C(O)CH$_3$), 26.8 (γ-CH_2), 54.9 (SiCH$_2$O), 171.7 (C(O)CH$_3$); ^{29}Si, 14.9. Anal. Calcd for C$_{10}$H$_{18}$O$_4$Si: C, 52.15; H, 7.88. Found: C, 52.0; H, 7.9.

1,1-Bis(acetoxymethyl)-1-silacyclohexane, (CH$_2$)$_5$Si(CH$_2$OAc)$_2$ (11). This compound was synthesized from 1,1-bis(chloromethyl)-1-silacyclohexane[16] (10.0 g, 50.7 mmol), sodium acetate (12.5 g, 152 mmol), and N,N-dimethylformamide (80 mL) to give **11** in 87% yield as a yellowish liquid (10.8 g, 44.2 mmol). Bp.: 90 °C/0.2 mbar. NMR (CDCl$_3$): ^{1}H, δ 0.67−0.72 (m, 4 H, β-CH_2), 1.34−1.41 (m, 2 H, δ-CH_2), 1.61−1.69 (m, 4 H, γ-CH_2), 1.99 (s, 6 H, C(O)CH_3), 3.87 (s, 4 H, SiCH_2O); ^{13}C, δ 8.5 (β-CH_2), 20.7 (C(O)CH$_3$), 24.0 (δ-CH_2), 29.3 (γ-CH_2), 54.0 (SiCH$_2$O), 171.6 (C(O)CH$_3$); ^{29}Si, −7.7. Anal. Calcd for C$_{11}$H$_{20}$O$_4$Si: C, 54.07; H, 8.25. Found: C, 53.7; H, 8.1.

Results and Discussion

Syntheses. The acyclic carbon-based nitratomethyl compounds Me$_3$CCH$_2$ONO$_2$[3] (**1a**), Me$_2$C(CH$_2$ONO$_2$)$_2$[3] (**2a**), and MeC(CH$_2$ONO$_2$)$_3$[3] (**3a**) were synthesized according to Scheme 2 by treatment of the corresponding commercially available hydroxymethyl compounds with fumic nitric acid. The related cyclic nitratomethyl compounds, (CH$_2$)$_4$C(CH$_2$ONO$_2$)$_2$ (**4a**) and (CH$_2$)$_5$C(CH$_2$-ONO$_2$)$_2$ (**5a**), were obtained analogously (Scheme 2; for the synthesis of the corresponding hydroxymethyl compounds, (CH$_2$)$_4$C(CH$_2$OH)$_2$ and (CH$_2$)$_5$C(CH$_2$OH)$_2$, see ref 35). The nitrates **1a−5a** were synthesized by treatment of the corresponding alcohols with an excess of fumic nitric acid and acetic anhydride at 0 °C, and the reaction mixtures were then stirred at ambient temperature, followed by an aqueous workup. In the case of **3a**, the precursor MeC(CH$_2$OH)$_3$ was treated with an excess of fumic nitric acid at 0 °C using dichloromethane as the solvent, followed by stirring of the reaction mixture at ambient temperature and subsequent aqueous workup. Compounds **1a−5a** were isolated in 82−88% yield without any byproduct. Several other syntheses of these compounds are known[36] but in anticipation of the syntheses of their corresponding sila-analogues, this gentle and non-oxidizing synthetic route was used.

For the synthesis of the (nitratomethyl)silanes **1b−5b**, the corresponding (hydroxymethyl)silanes were synthesized as precursors by using the method described in refs 12 and 15. The syntheses of the bis(hydroxymethyl)-silanes **6−8** by using this particular synthetic pathway were not reported before and therefore shall be briefly described. Compounds **6−8** were synthesized according to Scheme 3, starting from the respective bis(chloro-methyl)silanes.[16] Thus, treatment of Me$_2$Si(CH$_2$Cl)$_2$, (CH$_2$)$_4$Si(CH$_2$Cl)$_2$, and (CH$_2$)$_5$Si(CH$_2$Cl)$_2$ with sodium acetate in N,N-dimethylformamide furnished the corresponding bis(acetoxymethyl)silanes **9−11** (76−87% yield), which upon methanolysis, in the presence of acetyl chloride as a source for the formation of catalytic amounts of hydrogen chloride, yielded the corresponding bis(hydroxy-methyl)silanes **6−8** (60−73% yield).

Scheme 2. Synthesis of the Carbon-Based Nitratomethyl Compounds **1a−5a**, Starting from the Corresponding Hydroxymethyl Derivatives
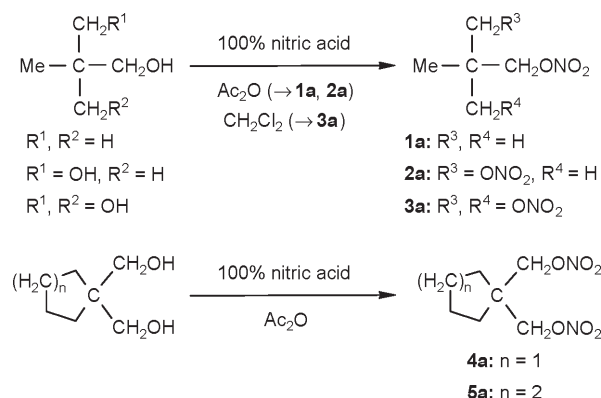
Scheme 3. Synthesis of the Bis(hydroxymethyl)silanes **6−8**, Starting from the Corresponding Bis(chloromethyl)silanes
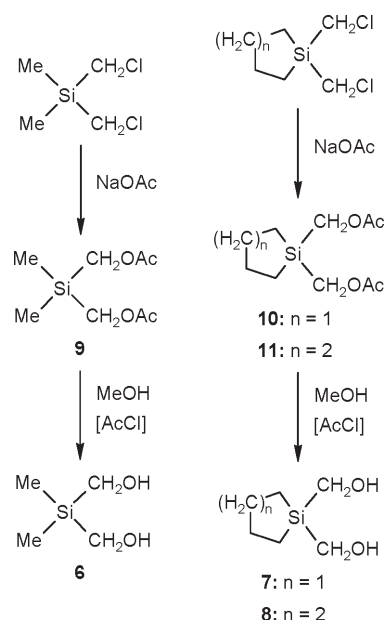
For an alternative synthesis of the (nitratomethyl)-silanes **1b−3b**, the corresponding (iodomethyl)silanes were used as precursors. Me$_3$SiCH$_2$I was commercially available, and Me$_2$Si(CH$_2$I)$_2$ was prepared from the commercially available bis(chloromethyl)silane Me$_2$Si-(CH$_2$Cl)$_2$.[37,38] MeSi(CH$_2$I)$_3$ was synthesized as reported in the literature.[15]
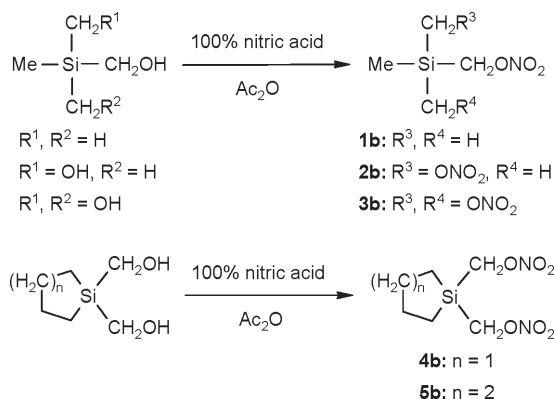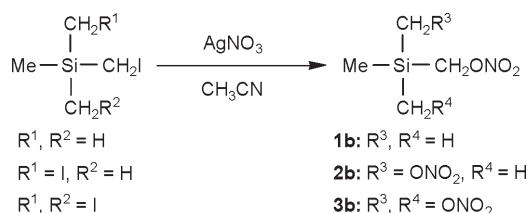
The silicon-based nitratomethyl compounds **1b−5b** were synthesized analogously to their corresponding carbon analogues **1a−5a** by treatment of the corresponding hydroxymethyl derivatives with an excess of fuming nitric acid and acetic anhydride (Scheme 4).[7] Compounds **1b−3b** were additionally prepared by treatment of the corresponding iodomethyl derivatives with an excess of silver nitrate at 0 °C using acetonitrile as the solvent, followed by stirring of the reaction mixture at ambient temperature and subsequent extraction with pentane (Scheme 5). In the case of **2b−5b**, the first approach (nitration of the corresponding alcohols) was found to

(35) Domin, D.; Benito-Garagorri, D.; Mereiter, K.; Fröhlich, J.; Kirchner, K. *Organometallics* **2005**, *24*, 3957−3965.

(36) Agrawal, J. P.; Hodgson, R. D. *Organic Chemistry of Explosives*; John Wiley & Sons: Chichester, 2007, pp 87−123.

(37) Roberts, J. D.; Dev, S. *J. Am. Chem. Soc.* **1951**, *73*, 1879−1880.

(38) Vivet, B.; Cavelier, F.; Martinez, J. *Eur. J. Org. Chem.* **2000**, 807−811.

Scheme 4. Synthesis of the Silicon-Based Nitratomethyl Compounds **1b−5b**, Starting from the Corresponding Hydroxymethyl Derivatives

Scheme 5. Synthesis of the Silicon-Based Nitratomethyl Compounds **1b−3b**, Starting from the Corresponding Iodomethyl Derivatives

be the best synthetic method. In contrast, for the synthesis of **1b** the second method turned out to be more advantageous. Compounds **1b−5b** were isolated in 80−96% yield.

NMR Analyses. The carbon-based nitratomethyl compounds **1a−5a** and their corresponding sila-analogues **1b−5b** show quite similar trends in the chemical shifts of their ^{1}H NMR resonances. Compared to the acyclic carbon compounds **1a−3a**, their sila-analogues **1b−3b** are high-field shifted in the ^{1}H NMR spectra. Especially the resonances of the methyl protons are strongly influenced by the respective α-atoms, the central carbon or silicon atom. The β-CH_2 proton resonances are strongly high-field shifted for the silicon compounds **1b−3b** compared to those of their corresponding carbon analogues **1a−3a**. The resonances of the hydrogen atoms of the ring systems of the cyclic carbon compounds **4a** and **5a** differ from those of the sila-analogues **4b** and **5b**, respectively. For **5a** only one broad ^{1}H resonance signal was observed, because of overlapping of the different CH_2 resonances of the ring system, whereas in the case of **5b** three clearly defined multiplet structures were observed. In detail, the δ-CH_2 ^{1}H resonances of **5b** are only slightly influenced compared to those of **5a**, whereas the β-CH_2 resonances are strongly high-field shifted and the γ-CH_2 resonances low-field shifted compared to those of **5a**. In the case of the C/Si analogues **4a** and **4b**, the β-CH_2 ^{1}H resonances are not affected by the α-atom (C or Si). However, as in the case of **5a** and **5b**, the β-CH_2 protons of **4b** show strongly high-field shifted resonances compared to those of the carbon analogue **4a**. The ^{1}H resonances of the exocyclic CH_2 groups are quite similar for the cyclic C/Si pairs **4a/4b** and **5a/5b**, that is, they are only slightly influenced by the α-atom (C or Si). With increasing the number of the nitratomethyl groups, the proton

resonances are low-field shifted in both series of compounds. The influence of the alkyl substituents (methyl, butane-1,4-diyl, and pentane-1,5-diyl) on the proton resonances of the ElCH_2O groups of the bis(nitratomethyl) derivatives **2a**, **2b**, **4a**, **4b**, **5a**, and **5b** is small. In both cases (El = C or Si), the ElCH_2O ^{1}H resonances are low-field shifted for the cyclic derivatives (**4a**, **4b**, **5a**, and **5b**) compared to the acyclic dimethyl compounds **2a** and **2b**.

The ^{13}C NMR resonances of the C/Si pairs **1a/1b−5a/ 5b** are more influenced by the number of the nitratomethyl groups than the ^{1}H resonances. With increasing number of the nitratomethyl moieties, the CH_2 and CH_3 resonances exhibit a high-field shift of 3−4 ppm. In contrast, the central α-carbon atom shows a low-field shift when increasing the number of nitratomethyl groups. The ring size of the cyclic carbon compounds **4a** and **5a** exerts only a small influence on the ^{13}C NMR resonances of the CH_2O groups. The ring CH_2 groups of **4a** and **5a** are easier to distinguish in the ^{13}C than in the ^{1}H NMR spectra. The ^{13}C resonances of the central carbon atom (α-atom) are strongly affected by the alkyl substituents (methyl, butane-1,4-diyl, and pentane-1,5-diyl). The exchange of the central carbon by a silicon atom shifts the ^{13}C NMR resonances to higher field, with the same shifting tendencies as observed in the series of the carbon compounds **1a−5a**. Because of hyperconjugation and β-silyl effect,[39] the ^{13}C NMR resonances of the SiCH_3 groups are high-field shifted by 0 to −10 ppm.

The ^{14}N NMR resonances of the nitrato groups of the carbon compounds **1a−5a** are observed in a region between −41 and −45 ppm. The ^{14}N resonances of the corresponding sila-analogues **1b−5b** are shifted to lower field in a region between −34 and −41 ppm. In both series of compounds, high-field shifting is observed with increasing number of the nitratomethyl groups. The ring size of the C/Si pairs **4a/4b** and **5a/5b** has only a weak influence on the ^{14}N chemical shift, but a high-field shift of 3−4 ppm is observed for each additional nitratomethyl moiety.

The acyclic silicon compounds **1b−3b** show ^{29}Si NMR resonances in a region between 0.1 and −5.4 ppm, and high-field shifting is observed with increasing the number of the nitratomethyl groups. The ^{29}Si resonances of the silicon compounds **2b**, **4b**, and **5b** are strongly dependent on the nature of the alkyl substituent (**2b**, −1.2 ppm; **4b**, 13.7 ppm; **5b**, −6.5 ppm).

Physical Properties. The boiling, melting, and decomposition points of the C/Si pairs **1a/1b−5a/5b** were measured by differential scanning calorimetry (DSC) (Table 1). The acyclic carbon compounds **1a−3a** have boiling points in the temperature range 174−183 °C, but **2a** and **3a** already start to decompose at 160 °C. For the cyclic carbon compounds **4a** and **5a**, no boiling points could be determined because they start to decompose at 190 °C. For **2a** and **4a**, unexpectedly high melting points were observed (**2a**, ∼ 20 °C; **4a**, 23 °C). Compound **3a** has a melting point of ∼ −15 °C,[2] and **5a** becomes highly viscous upon cooling, but does not solidify at −18 °C.

The silicon compounds **1b−5b** decompose violently in the temperature range 85−107 °C, which is 80−95 °C

(39) Schraml, J. In *The Chemistry of Organic Silicon Compounds*; Rappoport, Z., Apeloig, Y., Eds.; John Wiley & Sons: Chichester, 2001; Vol. 3, pp 223−339.

lower in temperature compared to the corresponding carbon analogues **1a**−**5a** (Tables 1 and 2). Interestingly, the decomposition temperatures of the cyclic silicon compounds **4b** and **5b** are slightly lower than those for the acyclic derivatives **1b**−**3b**. This is in contrast to the corresponding carbon analogues **1a**−**5a**, which show slightly higher decomposition points for the cyclic compounds **4a** and **5a** compared to their acyclic derivatives **1a**−**3a**. The highest decomposition points of the silicon-based nitratomethyl compounds **1b**−**5b** were observed for **2b** and **3b** (ca. 107 °C). The boiling points of **1b**−**5b** could not be determined because of prior explosive decomposition. The silicon compounds **1b**−**5b** have lower melting points (**2b**, ∼ −10 °C; **3b**, −18 °C; **4b**, −18 °C; **5b**, ∼ 4 °C) than the corresponding carbon analogues, except for **5b** with a melting point of about 4 °C. Only **5b** crystallized at 4 °C in a refrigerator, whereas all the other compounds solidified at −18 °C in the freezer, except for compound **1b**, which remained liquid. The silicon-based nitratomethyl compounds can be stored at −18 °C (**1b**−**5b**) and 4 °C (**4b**, **5b**), respectively, without decomposition but decompose slowly at ambient temperature.

The decomposition of **1b** in dry trichloromethane at 25 °C, −4 °C, and −18 °C was studied by $^{29}Si\{^1H\}$ NMR spectroscopy as a function of time (Figure 1). The aliquots of **1b** were stored at 4 °C and −18 °C as pure substance (in air), and NMR samples were freshly prepared in dry trichloromethane after a period of time. The NMR spectra at ambient temperature were collected from one NMR sample prepared in dry trichloromethane, which was repeatedly measured after a period of time. After 10 days of storing **1b** at ambient temperature and air, about 20% (and after 60 days about 50%) was decomposed. The main decomposition product was unambiguously identified as hexamethyldisiloxane,[39] the formation of which is not understood at this time. At 4 °C after 24 days, about 20% of **1b** was decomposed to give hexamethyldisiloxane, but no significant decomposition was observed upon storing at −18 °C over a period of 24 days. The NMR samples were taken from pure substances for the series at 4 °C and −18 °C.

Friction and Impact Sensitivities. The experiments concerning the friction and impact sensitivities of the C/Si pairs **1a/1b**−**5a/5b** were performed according to BAM (*Bundesanstalt für Materialforschung and -prüfung*) standards.[19] The parent carbon compounds **1a**−**5a** were found to be much less sensitive toward impact and friction compared to their corresponding sila-analogues **1b**−**5b** (Table 3). Even the lowest sensitivity (impact and friction) observed for the silicon compounds (**1b**) is much higher than the highest sensitivity of the discussed carbon analogues (**3a**).[2] The impact sensitivities of the silicon compounds are in the range of the critical value of measurability of the BAM setup (< 0.5 J).

The number of the nitratomethyl groups is the most important factor influencing the friction sensitivity of the compounds studied. The cyclic silicon compounds **4b** and **5b** are less sensitive toward friction than the corresponding acyclic derivatives **1b**−**3b**, with **4b** (five-membered ring) showing a higher sensitivity toward friction than **5b** (six-membered ring). This might be due to the larger ring strain in the case of **4b**. Compounds **2a** and **4a** were measured as liquids, but spontaneous crystallization during the friction
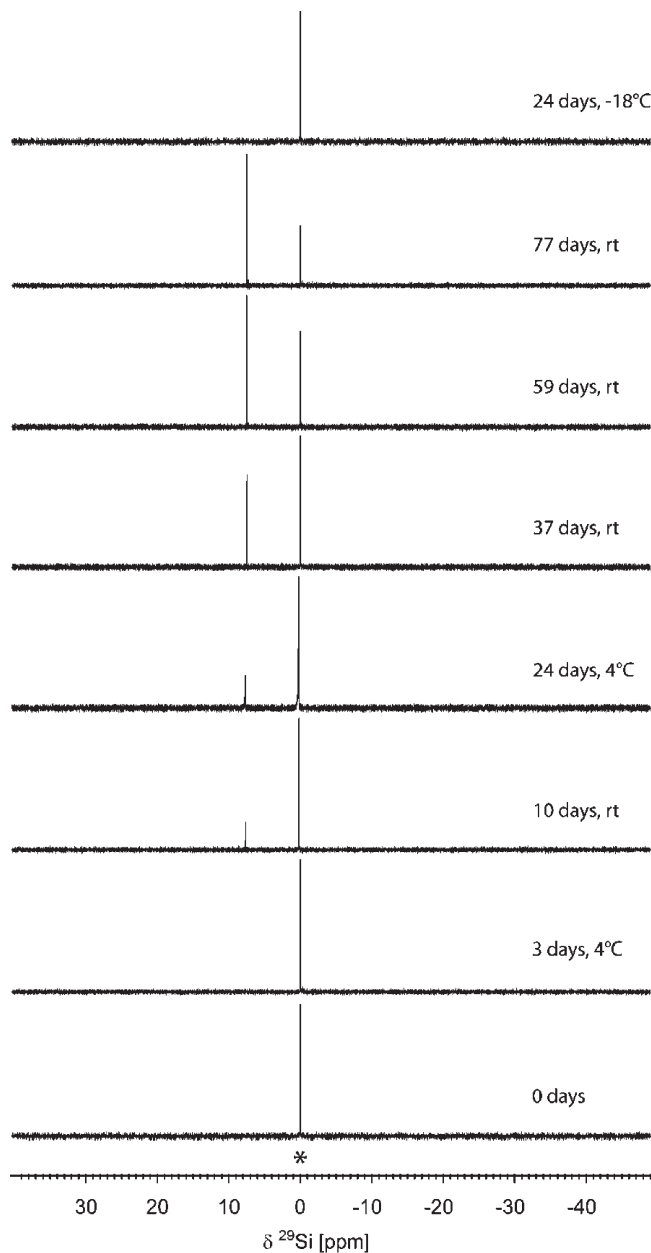

Figure 1. Decomposition of **1b** (*) at various temperatures (25 °C, 4 °C, and −18 °C) and as a function of time in dry CDCl₃ as monitored by $^{29}Si\{^1H\}$ NMR spectroscopy.

tests was observed, which would explain the higher sensitivity of the bis(nitratomethyl) compound **2a** compared to the tris(nitratomethyl) derivative **3a**.

Crystal Structure Analyses. The nitratomethyl compounds $Me_2C(CH_2ONO_2)$ (**2a**), $Me_2Si(CH_2ONO_2)_2$ (**2b**), $(CH_2)_4C(CH_2ONO_2)$ (**4a**), and $(CH_2)_5Si(CH_2ONO_2)$ (**5b**) and the silicon-containing precursors $(CH_2)_4Si(CH_2OH)_2$ (**7**) and $(CH_2)_5Si(CH_2OH)_2$ (**8**) were structurally characterized by single-crystal X-ray diffraction. The crystallographic data for **2a**, **2b**, **4a**, and **5b** are given in Table 4. The molecular structures of these compounds in the crystal are depicted in Figures 2−5; selected bond lengths and angles are listed in Tables 5 and 6. For the crystal structure analyses of the precursors **7** and **8**, see the Supporting Information.

The carbon-based nitratomethyl compound **2a** crystallizes in the monoclinic space group $P2_1/c$, with four

Table 3. Friction and Impact Sensitivities Measured for **1a−5a** and **1b−5b** (BAM Testing)

compound	1a	2a	3a	4a	5a	1b	2b	3b	4b	5b
friction [N][a]	> 360	> 96	> 108	> 108	> 120	> 64	< 5	< 5	< 5	> 36
impact [J][b]	> 100	> 100	> 15	> 100	> 100	> 1	< 0.5	< 0.5	< 0.5	< 0.5

[a] Measuring range, 5 N < x < 360 N. [b] Measuring range, 0.5 J < x < 100 J.

Table 4. Crystal Data and Details of the Structure Determinations of **2a**, **2b**, **4a**, and **5b**

	2a	2b	4a	5b
formula	$C_5H_{10}N_2O_6$	$C_4H_{10}N_2O_6Si$	$C_7H_{12}N_2O_6$	$C_7H_{14}N_2O_6Si$
M_r	194.15	210.23	220.19	250.29
T/K	100(2)	140(2)	100(2)	200(2)
$\lambda/Å$	0.71073	0.71073	0.71073	0.71073
crystal system	monoclinic	monoclinic	monoclinic	monoclinic
space group	$P2_1/c$	$P2_1/c$	$P2_1/n$	$P2_1/c$
crystal size/mm	0.15 × 0.18 × 0.03	0.1 × 0.1 × 0.02	0.21 × 0.17 × 0.06	0.2 × 0.2 × 0.2
$a/Å$	7.5819(5)	7.6671(3)	7.0159(6)	10.4017(9)
$b/Å$	10.5551(6)	11.0136(4)	9.6605(9)	6.7723(6)
$c/Å$	11.5215(7)	12.0510(5)	14.7399(9)	16.6297(14)
β/deg	106.530(7)	105.407(5)	91.061(6)	94.726(8)
$V/Å^3$	883.93(9)	981.04(7)	998.86(14)	1167.47(17)
Z	4	4	4	4
$\rho_{calc.}/g/cm^{-3}$	1.459	1.423	1.464	1.424
μ/mm^{-1}	0.135	0.243	0.129	0.217
$F(000)$	408	440	464	528
2θ range/deg	7.90−52.00	7.68−52.00	7.66−52.98	7.50−52.00
index ranges	$-9 \leq h \leq 9$	$-9 \leq h \leq 9$	$-8 \leq h \leq 8$	$-12 \leq h \leq 12$
	$-13 \leq k \leq 12$	$-13 \leq k \leq 16$	$-11 \leq k \leq 11$	$-8 \leq k \leq 8$
	$-12 \leq l \leq 14$	$-14 \leq l \leq 14$	$-18 \leq l \leq 18$	$-14 \leq l \leq 20$
reflections collected	4902	9722	6995	5355
reflections unique	1726 [$R_{int} = 0.0414$]	1936 [$R_{int} = 0.0200$]	1952 [$R_{int} = 0.0379$]	2254 [$R_{int} = 0.0955$]
parameters	118	128	184	145
GoF	0.959	1.180	0.859	0.990
R_1/wR_2 [$I > 2\sigma(I)$]	0.0411/0.0756	0.0301/0.0825	0.0329/0.0678	0.0588/0.0814
R_1/wR_2 (all data)	0.0786/0.0853	0.0406/0.0887	0.0711/0.0751	0.1686/0.1141
max/min residual electron density/e $Å^{-3}$	+0.201/−0.172	+0.326/−0.172	+0.151/−0.169	+0.315/−0.291
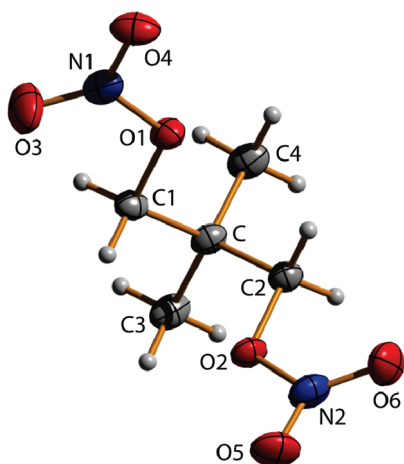
Figure 2. Molecular structure of **2a** in the crystal showing the atom labeling scheme. Thermal ellipsoids are shown at the 50% probability level.

Figure 3. Molecular structure of **2b** in the crystal showing the atom labeling scheme. Thermal ellipsoids are shown at the 50% probability level.

molecules in the unit cell, a calculated density of 1.459 g/cm^3, and a cell volume of 883.93(9) Å^3. As also observed for the cyclic derivative **4a** (monoclinic, space group $P2_1/n$, four molecules in the unit cell, density 1.464 g/cm^3), the bond lengths and angles of the C−CH$_2$−ONO$_2$ unit are in good agreement with the data obtained for PETN.[40] Only the CH$_2$−O bonds are slightly longer than a "normal"

C−O single bond (1.43 Å),[41] with bond lengths of approximately 1.46 Å (**2a**) and 1.45 Å (**4a**), respectively, but almost identical with the CH$_2$−O bond lengths observed for PETN.[40] The structure of the NO$_2$ group is quite similar to that observed for PETN and gaseous nitrogen dioxide. The lengths of the N−O bonds in this moiety are between those of a classic N−O single and double bond, in good agreement with PETN and gaseous nitrogen dioxide.[40,41]

The silicon-based nitratomethyl compound **2b** crystallizes in the monoclinic space group $P2_1/c$, with four

(40) Trotter, J. *Acta Crystallogr.* **1963**, *16*, 698−699.
(41) Cotton, F. A.; Wilkinson, G. *Advanced Inorganic Chemistry*, 5th ed.; John Wiley & Sons: New York; 1988, pp 321−323.
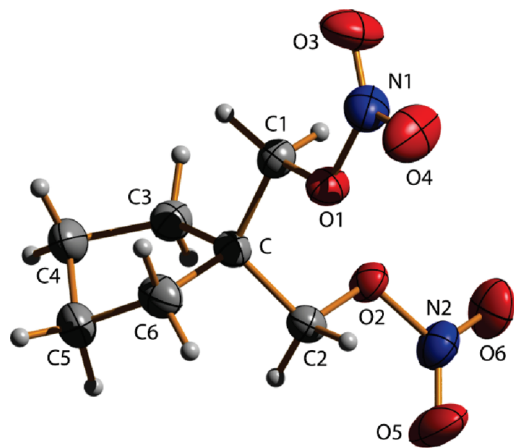
Figure 4. Molecular structure of **4a** in the crystal showing the atom labeling scheme and thermal ellipsoids at the 50% probability level.
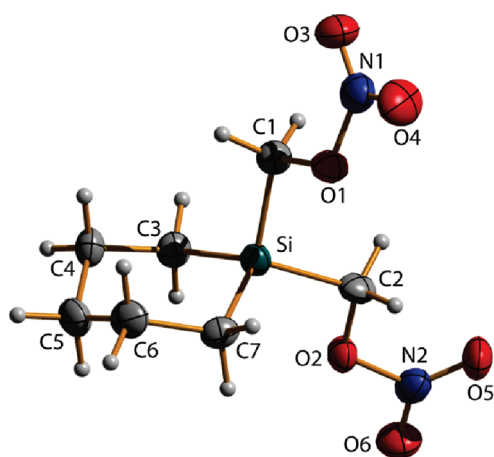

Figure 5. Molecular structure of **5b** in the crystal showing the atom labeling scheme. Thermal ellipsoids are shown at the 50% probability level.

molecules in the unit cell, a cell volume of 981.04(7) Å^3, and a density of 1.423 g/cm^3. The cyclic derivative **5b** crystallizes in the monoclinic space group $P2_1/c$, with four molecules in the unit cell, a cell volume of 1167.47(17) Å^3, and a density of 1.424 g/cm^3.

The bond lengths of these compounds are similar to those of their carbon analogues. The lengths of the CH_2-O bonds of the silicon compound **2b** [1.4512(13) and 1.4495(15) Å] are marginally shorter than the corresponding bond lengths of the carbon analogue **2a** [1.457(2) and 1.460(2) Å]. Also, the $O-NO_2$ bonds of the silicon compounds are slightly longer than those of the carbon analogues. In comparable moieties like the nitratomethyl groups of the C/Si analogues **2a** and **2b** the bond strength is inversely related to the bond length. Therefore, the $O-NO_2$ bonds of the silicon compound are probably slightly weaker than those of the carbon analogue, but like the situation in methyl nitrate.[42]

To identify whether there are attractive interactions between the silicon atoms and the bridging oxygen atoms of **2b** and **5b**, one could be tempted to compare the distance between them with the sum of their van der Waals radii.[43] However, in the case of geminal arrange-

ments this is not a valid comparison. Alternatives are the use of two-bond radii of Bartell[44] or, to be preferred, the one-angle radii of Glidewell.[45] The distances to be considered for **2b** [2.672(1)/2.690(1) Å] and **5b** [2.679(3)/2.723(3) Å] are surprisingly close to the sum of Glidewell's values for silicon (1.55 Å) and oxygen atoms (1.13 Å) at 2.68 Å. This indicates an absence of pronounced attractive $Si\cdots O$ interactions. Such attractive interactions between geminal silicon (acceptor) and donor atoms (O, N) are known to have significant or even dominating effects on molecular structures. Examples are the structures of SiON (e.g., $F_3SiONMe_2$)[46] and SiNN compounds (e.g., $F_3SiN\text{-}(Me)NMe_2$)[47]; this effect has been coined the α-effect in silicon chemistry. However, in simple systems containing SiCO units (e.g., F_3SiCH_2OMe),[48] which are more closely related to compounds **2b** and **5b**, such pronounced interactions have not been found for the structures of the molecular ground states. The very similar Si−C−O angles of **2b** and **5b** [105.55(8)−108.6(2)°] and the analogous C−O−C angles of **2a** and **4a** [106.55(14)−107.09(13)°] do also not support the interpretation of our data in terms of such kind of interactions.

NBO analyses were performed at the B3LYP/cc-pVDZ level of theory (Figures 6 and 7). The resulting data of the C/Si analogues **2a** and **2b** show no significant evidence for intramolecular $C\cdots O$ and $Si\cdots O$ interactions, respectively.

The NBO charge distributions of compounds **2a** and **2b** are remarkably different (see Figures 6 and 7). Specifically, the NBO charge of the quaternary central carbon atom of **2a** shows a negative value of −0.100 e (e = electron; −0.058 e for $C(CH_3)_4$). In contrast, the central silicon atom of **2b** shows a positive value of 1.754 e (1.782 e for $Si(CH_3)_4$). The values for the CH_3 carbon atoms of compound **2a** are clearly negative (−0.646 e), but the CH_2 carbon atoms show only a slightly negative charge (−0.090 e). The corresponding values of the silicon analogue **2b** show strongly negative charges at both the CH_3 (−1.175 e) and the CH_2 carbon atoms (−0.561 e). The NBO charges of the oxygen and nitrogen atoms of the nitrato moieties of **2a** and **2b** show almost no influence of the carbon/silicon exchange. The same holds true for the NBO charges of the hydrogen atoms of the C/Si analogues **2a** and **2b**.

The enthalpies of formation ($\Delta_f H°$) of the single molecules **1a−5a** and **1b−5b** were calculated at the CBS-4 M level of theory (Table 7). The enthalpy changes of the isodesmic reactions ($\Delta_r H°$) shown in Scheme 6 were obtained by the sum of $\Delta_f H°$ of the products (**1a−5a**, $Si(CH_3)_4$) minus the sum of $\Delta_f H°$ of the reactands (**1b−5b**, $C(CH_3)_4$).

(42) Cox, A. P.; Waring, S. *Trans. Faraday Soc.* **1971**, *67*, 3441–3450.
(43) Bondi, A. *J. Phys. Chem.* **1964**, *68*, 441–451.

(44) Bartell, L. S. *J. Chem. Phys.* **1960**, *32*, 827–831.
(45) Glidewell, C. *Inorg. Chim. Acta* **1975**, *12*, 219–227.
(46) (a) Mitzel, N. W.; Losehand, U. *Angew. Chem.* **1997**, *109*, 2897–2899. *Angew. Chem., Int. Ed. Engl.* **1997**, *36*, 2807–2809. (b) Losehand, U.; Mitzel, N. W. *Inorg. Chem.* **1998**, *37*, 3175–3182. (c) Mitzel, N. W.; Losehand, U. *J. Am. Chem. Soc.* **1998**, *120*, 7320–7327. (d) Mitzel, N. W.; Losehand, U.; Wu, A.; Cremer, D.; Rankin, D. W. H. *J. Am. Chem. Soc.* **2000**, *122*, 4471–4482. (e) Mitzel, N. W.; Vojinović, K.; Fröhlich, R.; Foerster, T.; Rankin, D. W. H. *J. Am. Chem. Soc.* **2005**, *127*, 13705–13713.
(47) (a) Mitzel, N. W. *Chem.—Eur. J.* **1998**, *4*, 692–698. (b) Vojinović, K.; McLachlan, L. J.; Hinchley, S. L.; Rankin, D. W. H.; Mitzel, N. W. *Chem.—Eur. J.* **2004**, *10*, 3033–3042.
(48) Mitzel, N. W. *Z. Naturforsch.* **2003**, *58b*, 759–763.

Table 5. Bond Lengths (Å) of **2a**, **2b**, **4a**, and **5b** in the Crystal

	2a (El = C)	**2b** (El = Si)	**4a** (El = C)	**5b** (El = Si)
N1−O1	1.3908(19)	1.4021(13)	1.3977(16)	1.406(4)
N2−O2	1.3954(18)	1.3927(14)	1.3900(16)	1.407(4)
N1−O3/4	1.2033(19)/1.2096(19)	1.1878(15)/1.2035(14)	1.1948(18)/1.2001(18)	1.201(4)/1.205(4)
N2−O5/6	1.211(2)/1.2106(19)	1.2154(17)/1.2005(17)	1.1938(18)/1.2022(18)	1.192(4)/1.210(4)
C1−O1	1.460(2)	1.4512(13)	1.4541(18)	1.447(4)
C2−O2	1.457(2)	1.4495(15)	1.4535(18)	1.446(4)
El−C1/2	1.528(2)/1.523(2)	1.8860(12)/1.8892(12)	1.517(2)/1.514(2)	1.875(4)/1.883(4)
El−C3	1.535(2)	1.8489(14)	1.549(2)	1.852(4)
El−C4	1.537(3)	1.8500(13)		
El−C6			1.550(2)	
El−C7				1.850(4)
C3−C4			1.524(2)	1.532(5)
C4−C5			1.514(3)	1.523(5)
C5−C6			1.514(2)	1.513(5)
C6−C7				1.538(5)

Table 6. Bond Angles (deg) of **2a**, **2b**, **4a**, and **5b** in the Crystal

	2a (El = C)	**2b** (El = Si)	**4a** (El = C)	**5b** (El = Si)
O3−N1−O4	129.01(17)	128.75(12)	129.24(15)	129.2(4)
O5−N2−O6	129.29(16)	129.32(13)	128.66(15)	128.7(4)
O1−N1−O3/4	118.29(16)/112.70 (16)	118.37(11)/112.88(11)	118.25(14)/112.51(15)	118.1(4)/112.6(4)
O2−N2−O5/6	118.04(17)/112.67(16)	112.38(12)/118.30(12)	118.42(15)/112.93(15)	118.6(4)/112.7(3)
N1−O1−C1	114.16(13)	114.40(9)	113.55(12)	114.5(3)
N2−O2−C2	113.92(13)	114.27(10)	113.63(13)	114.1(3)
El−C1−O1	106.55(14)	106.69(8)	106.68(13)	108.6(2)
El−C2−O2	106.61(14)	105.55(8)	107.09(13)	106.6(2)
C1−El−C2	112.02(14)	108.68(5)	112.37(12)	103.77(17)
C1−El−C3	106.75(15)	109.50(6)	107.89(14)	108.09(18)
C1−El−C4	110.16(15)	106.60(6)		
C1−El−C6			112.50(13)	
C1−El−C7				111.34(18)
C2−El−C3	110.73(15)	107.37(6)	112.09(13)	113.92(18)
C2−El−C4	106.73(15)	109.83(6)		
C2−El−C6			107.30(14)	
C2−El−C7				112.62(18)
C3−El−C4	110.49(15)	114.74(7)		
C3−El−C6			104.47(13)	
C3−El−C7				107.07(17)
El−C3−C4			105.84(15)	111.2(3)
C3−C4−C5			103.47(16)	113.6(3)
C4−C5−C6			102.34(15)	115.0(3)
C5−C6−C7				114.4(3)
El−C6−C5			104.94(14)	
El−C7−C6				110.6(3)
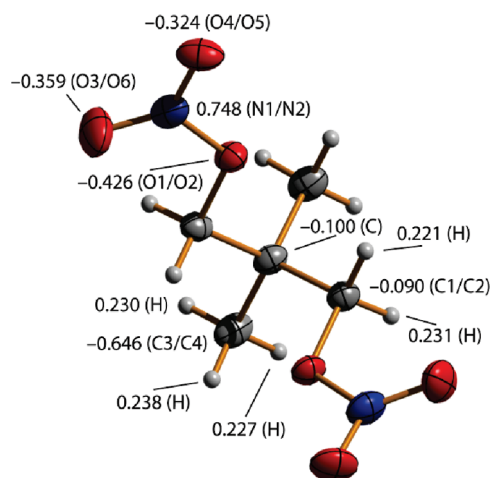
Figure 6. NBO charges of **2a**, calculated at the B3LYP/cc-pVDZ level of theory. All given values are in e (e = electron). The atom labels are shown in parentheses (see also Figure 2).


Figure 7. NBO charges of **2b**, calculated at the B3LYP/cc-pVDZ level of theory. All given values are in e (e = electron). The atom labels are shown in parentheses (see also Figure 3).

As can be seen from Table 7, all isodesmic reactions are exothermic ($\Delta_r H° < 0$). In detail, with increasing number of nitratomethyl groups, the value of $x\Delta_r H°$ increases. When comparing **1a** with **2a** and **1a** with **3a**, a doubling

Table 7. Enthalpies of Formation ($\Delta_f H°$, kcal/mol) for **1a−5a**, **1b−5b**, C(CH$_3$)$_4$, and Si(CH$_3$)$_4$ and Enthalpy Changes of the Isodesmic Reactions ($\Delta_r H°$, kcal/mol) of **1b−5b** to **1a−5a** (Scheme 6)

reaction	$\Delta_f H°$ (**1b−5b**)	$\Delta_f H°$ (C(CH$_3$)$_4$)	$\Delta_f H°$ (**1a−5a**)	$\Delta_f H°$ (Si(CH$_3$)$_4$)	$\Delta_r H°$
1b → 1a	−456720.0	−123857.1	−299182.9	−281398.6	−4.4
2b → 2a	−632040.4	−123857.1	−474507.9	−281398.6	−9.0
3b → 3a	−807358.9	−123857.1	−649830.6	−281398.6	−13.1
4b → 4a	−680527.0	−123857.1	−523000.7	−281398.6	−15.2
5b → 5a	−705155.8	−123857.1	−547624.0	−281398.6	−9.8

Scheme 6. Isodesmic Reactions of **1b−5b** with C(CH$_3$)$_4$ to **1a−5a** and Si(CH$_3$)$_4$
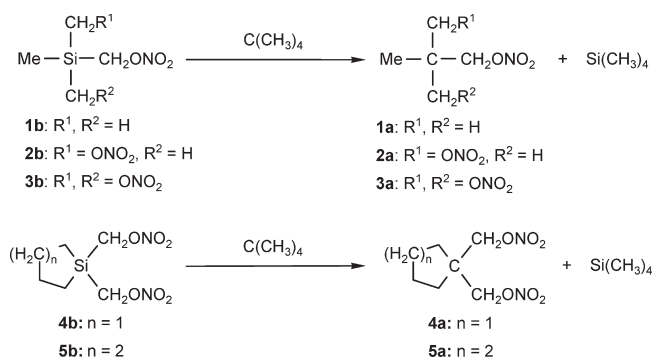
and a tripling, respectively, of the $\Delta_r H°$ value is observed. Comparison of the acyclic molecule **2a** with the related cyclic molecule **5a** (six-membered ring) reveals similar $\Delta_r H°$ values (−9.054 and −9.753 kcal/mol). In contrast, for the cyclic derivative **4a** (five-membered ring) a significantly higher $\Delta_r H°$ value (−15.209 kcal/mol) is observed. A possible explanation for this phenomenon is the increased ring strain in the case of **4a**.

The intramolecular Si···O distances between the silicon atoms and the bridging oxygen atoms observed for **2b** and **5b** are 2.672(1) and 2.723(3) Å, respectively, and this is the expected range for geminal silicon and oxygen atoms. The proximity of these atoms makes it plausible that the first step in the decomposition reaction is the highly exothermic formation of an Si−O bond and could promote the initial step for a chain reaction. Calculations for the decomposition pathway of Si(CH$_2$ONO$_2$)$_4$ confirm this view that the initial step of this process is the formation of an Si−O bond between the bridging oxygen atom and the central silicon atom.[8] This is in contrast to the decomposition pathway known for common nitrate ester explosives, where the homolytic O−NO$_2$ bond cleavage is the initial step.[3] However, it is in line with the finding of very shallow Si−C−N bending potentials observed for (aminomethyl)silanes, which can also be seen as contribution to the increased reactivity of such compounds at silicon.[49]

A closer look at the crystal structures of **2a** and **2b** provides a potential explanation for the relatively high melting points of these compounds. Six intermolecular interactions were found for both compounds, namely, those between the O1−N1−O3/4 and the O1′−N1′−O3′/4′ moieties. The resulting dimers and interactions are shown in Figure 8. The nitrato moieties of the molecular pairs are facing each other. In the case of **2a**, the shortest distance is the O1···O4′ contact [2.984(2) Å].

This distance is slightly shorter than the sum of the van der Waals radii (3.04 Å).[43] The O1···O4′ distance of **2b** is slightly longer than that of **2a** [3.066(1) Å] and is also slightly longer than the sum of the van der Waals radii. For both compounds, a second intermolecular contact is found between the oxygen atoms O2 and O4′, with O2···O4 distances of 2.862(2) Å (**2a**) and 2.921(1) Å (**2b**), respectively, which are somewhat shorter than the sum of the van der Waals radii (3.04 Å).[43] In addition, a third weak interaction between the nitrogen atom N2 and the oxygen atom O4′ was found. In the case of **2a**, this distance is 2.921(1) Å which is slightly shorter than the sum of the van der Waals radii (3.07 Å).[43] In the case of **2b**, the N2···O4′ distance amounts to 3.123(2) Å.

Gas Electron Diffraction Studies. The molecular structures of the C/Si analogues **1a** and **1b** were determined in the gas phase by gas electron diffraction (GED), aided by ab initio calculations using various theoretical models. The gas-phase structures of **1a** and **1b** are shown in Figures 9 and 10.

GED Molecular Models. On the basis of the ab initio calculations, the molecular models for **1a** and **1b** were constructed using overall C_s symmetry. In addition to this assumption of molecular symmetry, local C_{3v} symmetry was assumed for both the ElMe$_3$ group (El = C, Si) and each individual methyl group. Finally, on the basis of the relatively small scattering intensity for hydrogen, the hydrogen atoms in the CH$_2$ bridge were positioned with equal El−C−H (El = C, Si) and O−C−H angles, while the C−H distance in the CH$_2$ bridge was assumed to be equal to that of the methyl groups. Using this combination of assumptions, the total number of internal coordinates for each compound was reduced from 54 to 14, as shown in Tables 8 and 9. The atom numbering schemes used for the molecular models, corresponding to the descriptions in Tables 8 and 9, are shown in Figures 9 and 10. The only difference between the models for the two compounds, other than in the descriptions due to the exchange of carbon for silicon, was that the C−O and N−O bond lengths were described by an average and difference for **1a**, but were included as independent parameters for **1b**.

GED Refinements. The experimental molecular-intensity and radial-distribution curves for **1a** and **1b** are shown in Figures 11−14, with the refined difference curves shown at the bottom of each figure. The refinements were performed along the lines of the SARACEN method,[50] which places flexible restraints on parameters that are not well resolved from the GED experiment, with

(49) Mitzel, N. W.; Vojinović, K.; Foerster, T.; Robertson, H. E.; Borisenko, K. B.; Rankin, D. W. H. *Chem.—Eur. J.* **2005**, *11*, 5114−5125.

(50) (a) Blake, A. J.; Brain, P. T.; McNab, H.; Miller, J.; Morrison, C. A.; Parsons, S.; Rankin, D. W. H.; Robertson, H. E.; Smart, B. A. *J. Phys. Chem.* **1996**, *100*, 12280−12287. (b) Mitzel, N. W.; Rankin, D. W. H. *Dalton Trans.* **2003**, 3650−3662.
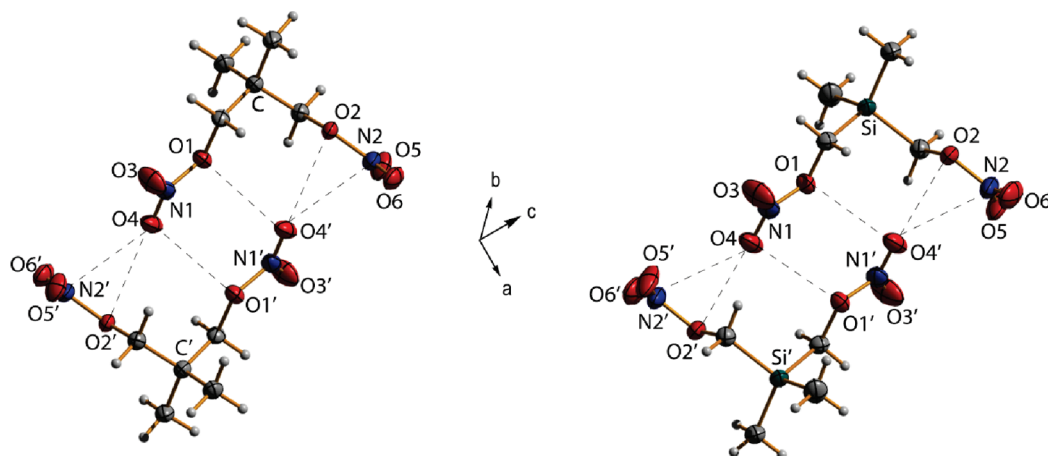
Figure 8. Aggregation motifs of pairs of molecules in the crystals of **2a** (left) and **2b** (right). The contacts O1···O4′, O2···O4′, and N2···O4′ are shown as dashed lines.
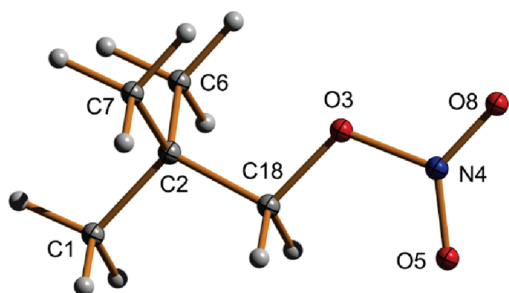

Figure 9. Molecular structure of **1a** in the gas phase showing the atom labeling scheme used for the GED model.
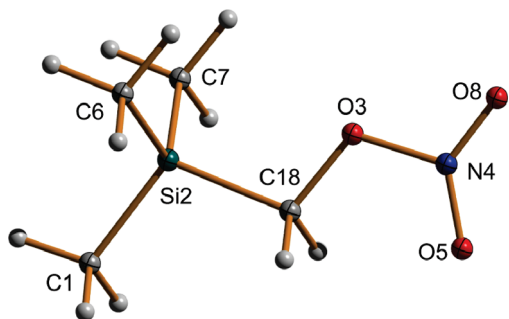

Figure 10. Molecular structure of **1b** in the gas phase showing the atom labeling scheme used for the GED model.

the value of the restraint being taken from theory and the uncertainty estimated by the convergence of the calculations (a strict interpretation of the SARACEN method would require the full number of independent parameters to be included in the model, but in this case we have made use of the assumptions mentioned above). All 14 independent parameters for both **1a** and **1b** were therefore refined as shown in Tables 8 and 9. Seven of these 14 parameters were refined unrestrained for **1a** and eight in the case of **1b**, the difference being that the C−O and N−O distances for **1b** were refined independently, whereas for **1a** they were included as an average and a difference, the latter of which was restrained. Amplitudes of vibration were also refined for both molecules, but those corresponding to distances under a single peak in the respective radial-distribution curve (RDC, see

Figures 11 and 13) were grouped together with fixed relative amplitudes. Restraints were also applied to all refined amplitudes, and for **1b** restraint uncertainties of 10% of the calculated values were applied, while those for **1a** were set to 10% for distances less than 4.5 Å and 20% for distances greater than 4.5 Å. The full lists of interatomic distances, amplitudes of vibration, and distance corrections for the r_{h1} refinements, including details of which amplitudes were tied together, are provided as Supporting Information.

The refinement of **1a** yielded a good fit of the experimental to theoretical intensities for both the r_g and r_{h1} structure types, as can be seen from the low R factors (R_G) of 4.7% and 5.2%, respectively. In the case of **1b**, the relatively low vapor pressure at room temperature required longer exposure times and a higher beam current than have been found to be optimum, and the data are correspondingly noisier than for **1a** and in previous GED structure investigations using this combination of apparatus and refinement techniques.[26,51] The resulting R factors of 16.4% and 14.9% for the respective r_g and r_{h1} structure types are higher than might be expected; however, the quality of the fit can also be judged by the appearance of the molecular-intensity and radial-distribution curves (Figures 13 and 14). In particular, the residuals of the molecular-intensity curves can be seen to be randomly distributed, indicating that the higher R factor is due to a lower signal-to-noise ratio rather than a refinement problem. Curiously, the standard deviations for the refined parameter values of **1a** and **1b** (Tables 8 and 9) are similar to one another, but from the preceding discussion it would be expected that the uncertainties for **1b** should be larger than those for **1a**. However, comparison of the RDCs (Figures 12 and 14) reveals that the structure of **1b** may be marginally better resolved by GED: While there are nine distinct peaks in the RDC for both compounds, the RDC for **1a** exhibits only one additional weak shoulder at about 3 Å, but the RDC for **1b** also contains two large shoulders at about 1.4 and 2.7 Å, as well as a small shoulder at 3.4 Å. Thus, the lower signal-to-noise ratio observed for **1b** is expected to be counterbalanced by

(51) Hagemann, M.; Berger, R. J. F.; Hayes, S. A.; Stammler, H.-G.; Mitzel, N. W. *Chem.—Eur. J.* **2008,** *14,* 11027–11038.

Table 8. Details of the Independent Parameters Used in the GED Refinement of **1a**, Refined Parameter Values, Calculated Values Obtained at the RI-MP2/TZVPP Level of Theory, and Applied Restraints[a]

	parameter description	GED r_g	GED r_{h1}	MP2 r_e	restraint uncertainty
p_1	r C−C average	1.539(1)	1.538(1)	1.525	
p_2	r C−O, N−O3 average	1.430(2)	1.429(2)	1.422	
p_3	r C−O, N−O3 difference	0.040(4)	0.035(4)	0.033	0.010
p_4	r N−O ×2 mean[b]	1.211(1)	1.210(1)	1.208	
p_5	r C−H	1.117(2)	1.114(2)	1.090	0.010
p_6	∠ C(Me)−C−C(Me)	109.2(2)	108.7(2)	109.9	
p_7	∠ C−C−O	106.3(3)	106.9(3)	106.9	
p_8	∠ C−O−N	113.6(3)	113.2(3)	113.2	
p_9	∠ O5−N−O8	132.0(6)	128.7(6)	130.0	
p_{10}	∠ H−C−H	111.0(3)	110.8(1)	108.3	1.0
p_{11}	r C−C difference[c]	0.002(4)	0.003(4)	0.005	0.005
p_{12}	CMe₃ tilt[d]	4.4(2)	3.7(2)	2.5	1.0
p_{13}	∠ O3−N−O difference[e]	4.7(5)	3.4(5)	4.4	1.0
p_{14}	r N−O ×2 difference[f]	0.008(4)	0.004(4)	0.006	0.005
	R factor (R_G)	4.7%	5.2%		

[a] All distances are in Å and angles are in deg. The two sets of parameter values for the GED refinement, r_g and r_{h1}, correspond to different approaches to accounting for vibrational motion. The r_g structure is a vibrational average, while the r_{h1} structure is an approximation to an equilibrium structure, r_e. [b] Average of N−O5 and N−O8. [c] C−C(Me) minus C−C18. [d] Defined as a decrease in the C1−C2−C18 angle with respect to that required for C_{3v} symmetry. [e] O3−N−O5 minus O3−N−O8. [f] N−O5 minus N−O8.

Table 9. Details of the Independent Parameters Used in the GED Refinement of **1b**, Refined Parameter Values, Calculated Values Obtained at the RI-MP2/TZVPP Level of Theory, and Applied Restraints[a]

	parameter description	GED r_g	GED r_{h1}	MP2 r_e	restraint uncertainty
p_1	r Si−C mean	1.883(1)	1.882(1)	1.879	
p_2	r C−O	1.447(5)	1.437(4)	1.433	
p_3	r N−O3	1.426(4)	1.435(3)	1.425	
p_4	r N−O ×2 mean[b]	1.208(1)	1.206(1)	1.206	
p_5	r C−H	1.104(3)	1.103(3)	1.090	0.010
p_6	∠ C(Me)−Si−C(Me)	110.9(4)	110.7(4)	111.2	
p_7	∠ Si−C−O	107.1(3)	108.3(3)	105.4	
p_8	∠ C−O−N	113.0(4)	113.6(4)	113.4	
p_9	∠ O5−N−O8	131.6(7)	131.3(7)	130.6	
p_{10}	∠ H−C−H	109.9(4)	109.5(3)	108.0	1.0
p_{11}	r Si−C difference[c]	0.033(3)	0.033(3)	0.034	0.005
p_{12}	SiMe₃ tilt[d]	2.8(6)	1.6(5)	1.3	1.0
p_{13}	∠ O3−N−O difference[e]	5.9(5)	5.2(5)	4.6	1.0
p_{14}	r N−O ×2 difference[f]	0.006(3)	0.005(3)	0.003	0.005
	R factor (R_G)	16.4%	14.9%		

[a] All distances are in Å and angles are in deg. The two sets of parameter values for the GED refinement, r_g and r_{h1}, correspond to different approaches to accounting for vibrational motion. The r_g structure is a vibrational average, while the r_{h1} structure is an approximation to an equilibrium structure, r_e. [b] Average of N−O5 and N−O8. [c] Si−C18 minus Si−C(Me). [d] Defined as a decrease in the C1−Si−C18 angle with respect to that required for C_{3v} symmetry. [e] O3−N−O5 minus O3−N−O8. [f] N−O5 minus N−O8.
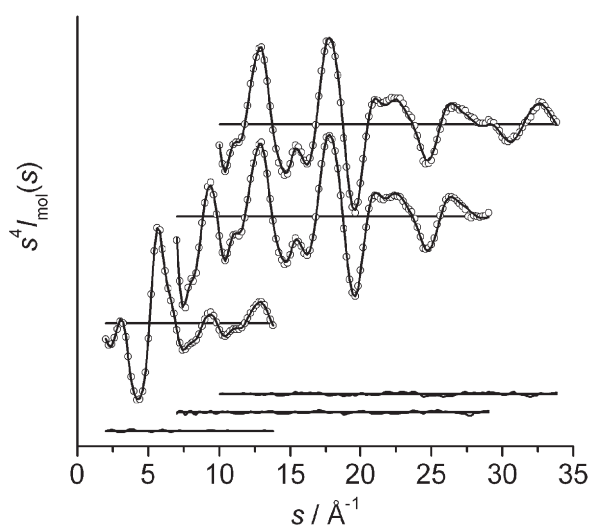
Figure 11. Experimental (O), theoretical, and difference (experimental minus theoretical) molecular-intensity curves for **1a**.

an increase in the structural information inherent in its electron diffraction pattern, compared to **1a**.

Discussion of the Gas-Phase Geometries. A selection of important geometric parameters for **1a** and **1b** are listed in Table 10, showing the convergence of the calculated structures, alongside the experimental GED structures, the latter being determined using both the r_g and the r_{h1} models for vibrational motion.[52] Comparison of the calculated and experimental values indicates that the Me₃ElCH₂ groups (El = C, Si) are reasonably well described by HF theory, with only small changes in the values of these parameters when improving the theoretical treatment by applying MP2 theory. In contrast, HF

(52) An internuclear distance obtained directly from the GED data, r_a, is the harmonic mean and can be converted to the arithmetic mean, r_g, using the root-mean-squared amplitude of vibration, u: $r_g \approx r_a + u^2/r$. Distance corrections, k, are also regularly applied in GED refinements to account for the 'shrinkage' effect. When the vibrational motion is considered to be harmonic with curvilinear trajectories, the resulting distances and distance corrections are termed r_{h1} and k_{h1}, respectively.
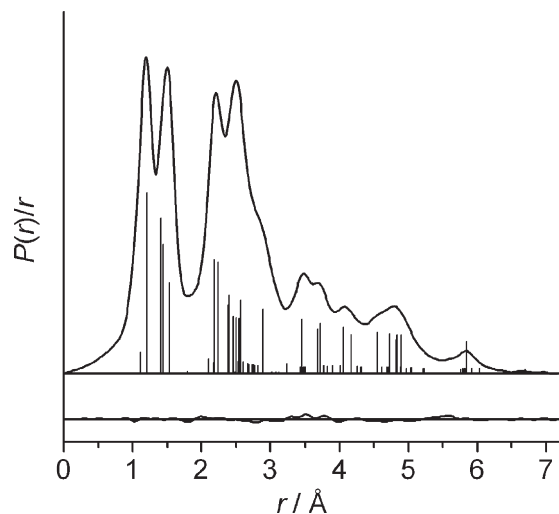
Figure 12. Experimental and difference (experimental minus theoretical) radial-distribution curves for **1a**. Prior to Fourier transformation, the molecular-intensity data were multiplied by $s \cdot \exp[-0.00002s^2/(Z_N - f_N)(Z_O - f_O)]$ and the s-range was extended to 0 and to 36 Å^{-1} by model data.
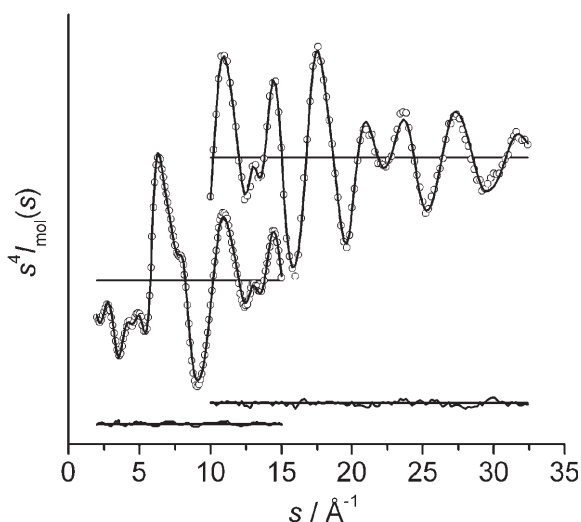

Figure 13. Experimental (○), theoretical, and difference (experimental minus theoretical) molecular-intensity curves for **1b**.

theory appears to have severe limitations with regard to the treatment of the nitrato group. The terminal N−O bonds are significantly elongated by applying MP2 theory, by more than 3 pm when the geometries calculated with identical basis sets are compared. The largest discrepancy between the HF and MP2 geometries of **1a** and **1b** is in the length of the N−O3 bond, which is lengthened by 0.081 Å (**1a**) and 0.095 Å (**1b**), respectively. Such a large difference between the HF and MP2 method would normally cast doubt on the accuracy of the MP2 geometry; however, the N−O bond lengths determined by GED agree very well with those determined by the MP2 method (although the differences between the N−O5 and N−O8 distances were restrained to the MP2 values).

The reliability of the GED results can be assessed by the agreement between the two models (r_g and r_{h1}) used to describe the vibrational motion, as well as the standard deviations from the least-squares fit. The agreement between the two models is reasonably good for all bond distances, the largest discrepancies for r_{C-O} being 0.009 Å
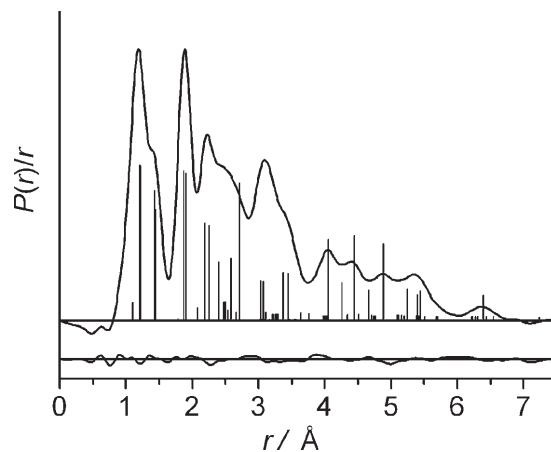

Figure 14. Experimental and difference (experimental minus theoretical) radial-distribution curves for **1b**. Prior to Fourier transformation, the molecular-intensity data were multiplied by $s \cdot \exp[-0.00003s^2/(Z_{Si} - f_{Si})(Z_O - f_O)]$ and the s-range was extended to 0 and to 36 Å^{-1} by model data.

Table 10. Selected Structural Parameters for **1a** and **1b** as Determined Experimentally by GED and Calculated by Theory[a]

method	HF/6-31G*[b] r_e	HF/[c] r_e	MP2/[c] r_e	GED r_g	GED r_{h1}
				Compound **1a**	
r C−H	1.085	1.083	1.090	1.117(2)	1.111(3)
r C−C(Me)	1.536	1.533	1.526	1.540(1)	1.539(1)
r C−C18	1.530	1.528	1.521	1.538(3)	1.535(3)
r C−O	1.439	1.435	1.438	1.450(3)	1.441(3)
r N−O3	1.327	1.324	1.405	1.410(2)	1.408(2)
r N−O5	1.187	1.179	1.211	1.215(2)	1.213(2)
r N−O8	1.179	1.170	1.205	1.207(2)	1.208(2)
∠ C−C−O	107.4	107.9	106.9	106.3(3)	106.9(3)
∠ C−O−N	116.5	116.7	113.2	113.6(3)	114.0(3)
∠ O5−N−O8	127.9	127.8	130.0	132.0(6)	129.7(7)
				Compound **1b**	
r C−H	1.086	1.084	1.090	1.104(3)	1.103(3)
r Si−C(Me)	1.886	1.877	1.870	1.875(1)	1.874(1)
r Si−C18	1.919	1.913	1.905	1.908(3)	1.907(3)
r C−O	1.439	1.435	1.433	1.447(5)	1.437(4)
r N−O3	1.333	1.330	1.425	1.426(4)	1.435(3)
r N−O5	1.185	1.177	1.207	1.211(2)	1.208(2)
r N−O8	1.179	1.171	1.204	1.205(2)	1.204(2)
∠ Si−C−O	106.6	107.4	105.4	107.1(3)	108.3(3)
∠ C−O−N	116.9	117.1	113.4	113.0(4)	113.6(4)
∠ O5−N−O8	128.0	128.0	130.6	131.6(7)	131.3(7)

[a] All distances r are in Å, angles ∠ are in deg, and the numbers in parentheses are one standard deviation in the last digit. For an explanation of the structure types, r_e, r_g, and r_{h1}, see ref 52. [b] 6-31G** was used for **1a**. [c] def2-TZVPP.

(**1a**) and 0.010 Å (**1b**), respectively. There is also a good agreement for most of the angles, with discrepancies mostly less than 1°, the exceptions being the O5−N−O8 angle for **1a** and the Si−C−O angle for **1b**, which therefore should be treated with some caution.

With regard to the increased friction and impact sensitivity of the silicon compound **1b** compared to its carbon analogue **1a**, the interesting parameters are the relative lengths of the N−O3 bonds and the Si−C−O and C−C−O angles. Both the experimental and calculated structures indicate a slight weakening of the N−O3 bond for the silicon compound **1b**, with an increase of about

0.02 Å for r_{N-O3}. The calculated structures of **1a** and **1b** also indicate a small (ca. 1°) contraction of the Si$-$C$-$O angle (**1b**) compared to the C$-$C$-$O angle (**1a**), but the experimentally established structures indicate a difference in the opposite direction. This parameter was not particularly well resolved in the GED structure of **1b**, as it was strongly dependent on the vibrational model. The observed discrepancy may be due to different dynamic behavior for **1a** and **1b** rather than a deficiency in the theoretical model for describing the static equilibrium geometries. In any case, the energy difference corresponding to such a small angle contraction would be minimal and the elongation of the O$-$NO$_2$ bond in **1b** is the only significant structural difference that might account for its greater instability.

Conclusion

The silicon-based nitratomethyl compounds Me$_2$Si(CH$_2$-ONO$_2$)$_2$ (**2b**), MeSi(CH$_2$ONO$_2$)$_3$ (**3b**), (CH$_2$)$_4$Si(CH$_2$ONO$_2$)$_2$ (**4b**), and (CH$_2$)$_5$Si(CH$_2$ONO$_2$)$_2$ (**5b**) were synthesized for the first time. In addition, the known derivative Me$_3$SiCH$_2$ONO$_2$ (**1b**) was resynthesized. The silicon compounds **1b**$-$**5b** were found to be much more sensitive toward friction and impact than their mostly known carbon analogues Me$_3$CCH$_2$-ONO$_2$ (**1a**), Me$_2$C(CH$_2$ONO$_2$)$_2$ (**2a**), MeC(CH$_2$ONO$_2$)$_3$ (**3a**), (CH$_2$)$_4$C(CH$_2$ONO$_2$)$_2$ (**4a**, new), and (CH$_2$)$_5$C(CH$_2$ONO$_2$)$_2$ (**5a**). The thermal stabilities of the silicon compounds **1b**$-$**5b** are approximately 80$-$95 °C lower than those of the corresponding carbon analogues **1a**$-$**5a**. Weak O$-$NO$_2$ bonds, strong C$-$O bonds, and the weaker Si$-$CH$_2$O bond of the silicon compounds are claimed to be responsible for the higher sensitivities compared to their corresponding carbon analogues. GED studies and calculations at different levels of theory established the gas phase structures of **1a** and **1b** in good agreement with the structural parameters obtained in single-crystal X-ray diffraction studies of **2a**, **2b**, **4a**, and **5b**. The carbon/silicon switch strategy has already been demon-strated to be a powerful tool for the development of novel drugs[17] and odorants[18] with unique properties. The studies presented here also clearly demonstrate the high potential of the sila-substitution concept (C/Si exchange) for the development of new silicon-based explosives (in this context see also refs 7 and 8), with properties that differ significantly from those of their corresponding carbon analogues.